Risk-Informed Resolution of GSI-191 at South Texas Project

Initial Quantification

Initial risk quantification estimates the core damage frequency (CDF) contribution of recirculation-related system failures caused by sump strainer or downstream fuel assembly blockage and at South Texas Project to be 4.96×10^{-7} events per calendar year. Estimates for LERF contribution were less than 1×10^{-9} per calendar year. Significant conservatisms support this initial estimate, but physical testing of chemical product formation and strainer bypass are planned to further reduce uncertainties. Safety issues having $\Delta CDF < 10^{-6}$/yr and $\Delta LERF < 10^{-7}$/yr fall in Risk Region III (very small changes) as defined by Regulatory Guide 1.174. A multidisciplinary analysis method was developed to integrate physical plant data and operational response with accident phenomenology in a software package that supports uncertainty analysis, parametric trade-off studies, and formal risk quantification when used in tandem with a site-wide PRA.

2/15/2011

Risk-Informed Closure of GSI-191 at South Texas Project Electric Generating Station

Executive Summary for 2011

The main objective of the Risk-Informed GSI-191 Closure Project is, "Through a risk-informed approach, establish a technical basis that demonstrates that the current design is sufficient to gain NRC approval to close the safety issues related to GSI-191 by the end of 2013." The results presented in this summary are the joint work of STP Risk Management, Los Alamos National Laboratories, The University of Texas at Austin, Texas A&M University, Alion Science and Technology, ABS Consulting, ScandPower, Mike Golay, The University of New Mexico, and KnF Consulting Services, LLC.

In the risk-informed approach, STP would seek exemption from certain requirements of 10 CFR 50.46 if the risk associated with the fibrous insulation installed in the STP containment buildings is not risk significant. If we determine this insulation to pose a significant risk, we are committed to investigating plant modifications including insulation removal and other measures to preserve sufficient margins for nuclear safety.

The 2011 preliminary results show that the risk for fibrous insulation in containment is less than 1.0E-06 to CDF and less than 1E-09 to LERF, or non-risk significant per RG 1.174.

These mean results account for the uncertainties of more than 20 input parameters and the complementary execution of the physics-based (CASA Grande) model, thermal-hydraulics model, and PRA models. Although previous realistic testing has shown that chemicals are unlikely to affect the head loss significantly in STP debris beds (sump strainers and fuel assemblies), we have used an initial methodology that adds conservative head-loss estimates from chemicals. Including these estimates is believed to fully address NRC concerns raised in pre-licensing meetings related to sump chemistry.

This preliminary assessment of the CDF and LERF gives us confidence that the issues associated with fibrous insulation in the STP reactor

containment buildings will be further shown to be non-risk significant with adequate defense-in-depth and safety margins such that we will receive NRC approval to close GSI-191 by the end of 2013.

We will expand upon the project's technical contributions by including the uncertainties of more than 50 input parameters and the seamless integration of CASA Grande, new jet formation model, uncertainty propagation in the thermal-hydraulics models, and PRA analysis that takes into account existing plant operational procedures for each scenario requiring sump recirculation.

Table of Contents

List of Figures

List of Tables

Acronyms and Abbreviations

CAD	Computer Aided Design
CASA	Containment Accident Stochastic Analysis
CDF	Core Damage Frequency
	Cumulative Distribution Function
CCDF	Complementary Cumulative Distribution Function
CLI	Cold-leg injection
CS	Containment Spray
DEGB	Double Ended Guillotine Break
ECCS	Emergency Core Cooling System
EOP	Emergency Operating Procedures
FA	Fuel Assembly
GB	Giga Byte
GL	Generic Letter
gpm	gallon per minute
GSI	Generic Safety Issue
HLI	Hot-Leg Injection
LERF	Large Early Release Frequency
LHS	Latin Hypercube Sampling
LLC	Limited Liability Corporation
LOCA	Loss of Coolant Accident (Small, Medium, Large)
MOR	Model of Record
NIST	National Institute of Standards and Technology
NLHS	Nonuniform LHS
NPSH	Net Positive Suction Head
NRC	Nuclear Regulatory Commission
PDF	Probability Density Function
PLG	Pickard, Lowe, and Garrick
PRA	Probabilistic Risk Assessment
PRT	Pressurizer Relief Tank
PWR	Pressurized Water Reactor
PWROG	Pressurized Water Reactor Owners Group
RAM	Random Access Memory
RCS	Reactor Coolant System
RCP	Reactor Coolant Pump
RG	Regulatory Guide (also RegGuide)

ROY	Reactor Operating Year
RWST	Refueling Water Storage Tank
SI	Safety Injection
SRM	Staff Requirements Memo
SRV	Safety Relief Valve
STL	Stereolithographic
STP	South Texas Project
STPEGS	South Texas Project Electric Generating Station
STPNOC	South Texas Project Nuclear Operations Company
ULHS	Uniform Latin Hypercube Sampling
UQ	Uncertainty Quantification
WCAP	Westinghouse technical document numbering prefix
ZOI	Zone of Influence

Background and Objectives

Since its declaration as a generic safety issue in 2001, GSI-191: Assessment of Debris Accumulation on PWR Sump Performance has presented numerous challenges to final resolution. Complex phenomena ranging from high-energy thermodynamics to post-LOCA chemistry and their combined interactions with plant safety systems have made it difficult to identify a cost-effective resolution strategy based on deterministic bounding analyses of individual factors. It is unlikely a deterministic approach that does not explicitly account for the time-evolution of accident phenomena and the full range of realistic behavior will ever provide a satisfactory closure path. This has been the experience at STP.

The original scope of GSI-191 was limited to sump blockage considerations only, and the South Texas Project Electric Generating Station (STP) achieved quantifiable risk reductions in 2007 by installing large-surface-area strainers on each of the three independent containment recirculation sumps. However, more recent emphasis on assumed adverse chemical product formation and penetration of fibrous debris types into reactor fuel assemblies has expanded the list of sensitive performance measures and further compounded the conservatism inherent to separate-effect deterministic evaluations.

In keeping with the agency's commitment to move towards increasing risk informed regulation, the NRC issued Staff Requirements Memorandum "Staff Requirements – SECY-10-0113 – Closure Options For Generic Safety Issue-191, Assessment Of Debris Accumulation On Pressurized Water Reactor Sump Performance" (Ref. 1) directing the staff to consider GSI-191 resolution strategies including an Option 2:

> *"The staff should take the time needed to consider all options to a risk-informed, safety conscious resolution to GSI-191. While they have not fully resolved this issue, the measures taken thus far in response to the sump-clogging issue have contributed greatly to the safety of U.S. nuclear power plants. Given the vastly enlarged advanced strainers installed, compensatory measures already taken, and the low probability of*

challenging pipe breaks, adequate defense-in-depth is currently being maintained.

The operative words for Option 2 are innovation and creativity. The staff should fully explore the policy and technical implications of all available alternatives for risk informing the path forward. These alternatives include, but are not limited to, how 50.46a might impact this issue, and how the application of a "no-transition-break-size" approach might work."

STP volunteered to provide a test case by working with the staff to develop risk-informed closure strategies while preparing a site-specific licensing submittal. The objective of risk analysis is to examine the full spectrum of accident conditions ranging from predominant, but small accidents that are easily managed by safety systems up to and including extreme, but unlikely accidents that challenge the design basis. Corresponding distributions of plant performance ranging from successful accident mitigation up to exceedance of performance thresholds indicating possible core damage are developed, which are properly balanced by the initiating event frequencies. The combination of conservative, yet realistic, treatments of accident phenomenology and decision criteria based on precursors to possible system damage enables risk-informed insights without compromising the traditional safety basis. For this initial risk quantification, the plant performance metrics of head loss across the recirculation strainers and fiber deposition per fuel assembly were used to assess the risk of flow blockage leading to core damage during recirculation scenarios.

It is worth reemphasizing that a risk-informed analysis includes *all* scales of postulated accidents and the full spectrum of possible plant responses. Ideally, there should be no exclusive focus on "bounding" assumptions, no exclusive focus on "design basis" or "beyond design basis" assumptions, and no exclusive focus on "best estimate" assumptions. Every factor in the accident analysis should be described as accurately as possible by a statistical distribution that is consistent with available data, and so, factors with limited data support necessarily have wider uncertainties. Furthermore, the statistical methods used to sample and propagate these uncertainties should be unbiased in the sense that they neither exaggerate nor minimize the decision criteria. In practice, however, important elements of conservatism are always retained in order

to secure confidence in the final results and to ensure that safety decisions based on these results are robust with respect to improved understanding over time. Numerous conservatisms are retained in this initial quantification to maintain consistency with many regulatory assumptions while developing a robust toolset and exploring parameter sensitivities.

Operational risk is formally quantified at STP using a mature, site-wide probabilistic risk assessment (PRA), and common figures of merit for comparing incremental risk between safety concerns is contribution to core damage frequency (CDF), given in units of # of core damage events per reactor calendar year and large early release frequency (LERF). Both metrics are computed assuming the reactor is at power. Risks posed during plant shutdown will be investigated in the remaining years of the project. Regulatory Guide 1.174 - An Approach for Using Probabilistic Risk Assessment in Risk-Informed Decisions on Plant-Specific Changes to the Licensing Basis (RG 1.174 - Ref. 2) assigns safety issues with incremental (Δ) contributions to CDF of less than 10^{-6} per calendar year and to LERF less than 10^{-7} per reactor calendar year to Risk Region III. Issues in this region are determined to be "very small" and are generally acceptable without significant additional analysis.

It is the intent of STP to rigorously quantify the risk contribution to core damage and large early release of recirculation scenarios that are encompassed by GSI-191. Comparison of the risk analysis to the RegGuide 1.174 Region-III limit of $\Delta CDF < 10^{-6}$ per yr and $\Delta LERF < 10^{-7}$ per year will provide a basis for GSI-191 closure via exemption to certain requirements in 10 CFR 50.46. The terms ΔCDF and ΔLERF in the context of this work mean the difference in CDF and LERF between a hypothetically perfect containment building having no fibrous insulation and the existing plant design. If the final analysis exceeds the guideline, STP is considering large-scale replacement of fiberglass insulation that will be costly in terms of (1) purchase and installation, (2) occupational radiation dose, and (3) resources diverted from higher-priority safety concerns.

If the final analysis supports the designation of recirculation failure as a Risk Region-III event, preventative measures will be identified to address contributing factors that carry the largest potential impacts in the analysis, and no further plant modifications

will be required. Regardless of the quantitative findings, STP will use the risk analysis to prioritize specific actions and determine the degree of remediation that may be required. Thus, it is essential that all parties fully understand the theory, implementation methods and interpretation of a risk-informed decision process.

This report presents the findings in the first year, an initial quantification, of a 3-year study being conducted to fully assess the incremental CDF contributed by recirculation failures at STP, and explains the technical basis for these results. The tools and methods developed for this initial quantification will be refined and expanded to support risk-informed closure of GSI-191.

Findings

Initial quantification estimates the CDF increase (ΔCDF) above a hypothetical "perfectly insulated STP containment" from recirculation failure to be 4.96×10^{-7} and ΔLERF to be $3.01X10^{-10}$ events/yr including significant conservatisms. These estimates are below the thresholds defined by Regulatory Guide 1.174, which categorize recirculation failure as a Risk Region-III safety concern. The RegGuide states that plant changes that lie in Risk Region III are very small changes and requires that the cumulative effect on plant CDF and LERF be tracked (although at this low level, CDF and LERF do not have to be considered when making a change). Figure 1 below is an illustration of the STP incremental change on a reproduction of the risk-space figure in the RegGuide. The remainder of this report explains the technical basis for these initial results and explains the inherent conservatisms that have been retained in the preliminary study.

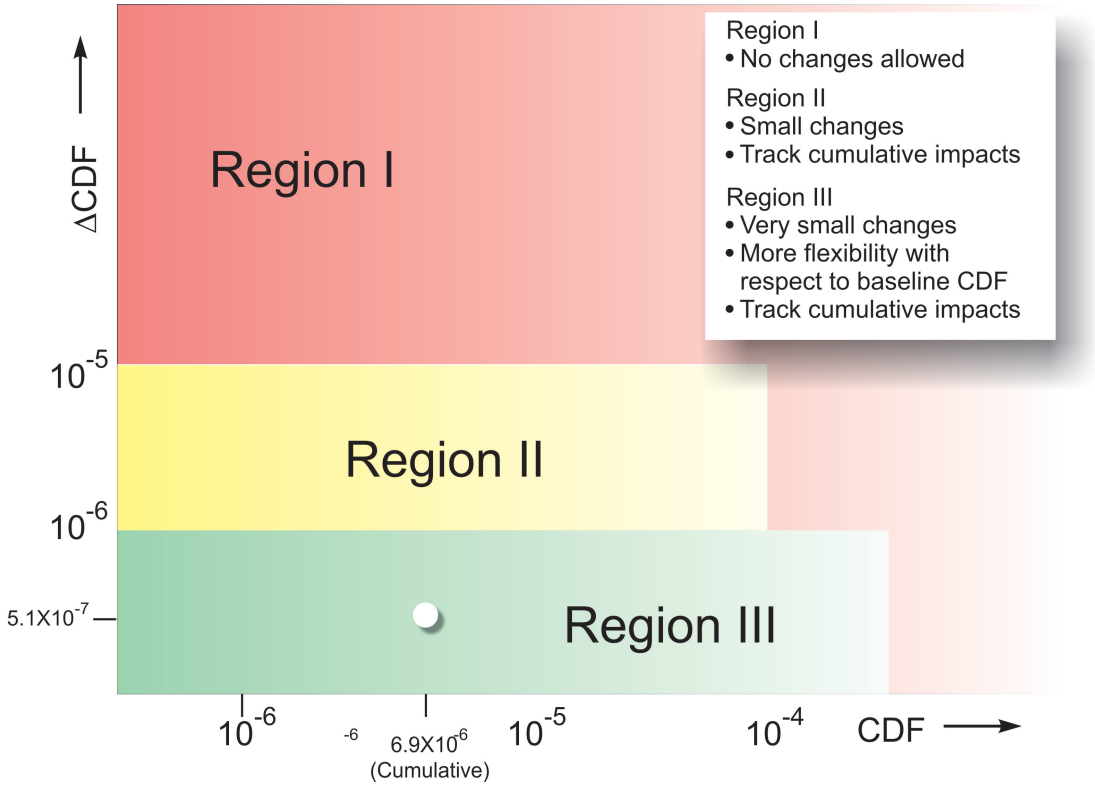

Figure 1. Risk regions defined by Regulatory Guide 1.174 for CDF with STP initial quantification.

Initial quantification has successfully merged team contributions in (1) weld rupture frequency, (2) system thermal hydraulics, (3) containment accident simulation, (4) as-built CAD technology, (5) statistical uncertainty quantification, (6) debris generation and transport, (7) plant emergency operations response, and (8) analysis of STP-specific and industry test data for chemical effects using a new software platform called CASA Grande. CASA (Containment Accident Stochastic Analysis) compiles a spectrum of time-dependent results for many thousands of postulated accident sequences in order to estimate the probability of sump failure for use in the plant-wide PRA. Initial quantification has identified several key uncertainties that will be the subject of phenomenology testing in Year 2, but no barriers have been encountered that will prevent further refinement and successful application of the methodology for risk quantification. CASA now enables convenient evaluation of parametric studies to

help STP, the industry and the NRC prioritize further research investments and perform risk-management comparisons.

One example of applied risk management at STP is shown in Figure 2, which illustrates the proportion of core damage contribution from various initiating events. On a risk priority basis at STP, dominant core damage events such as loss of offsite power and external events (high winds, flood, and so forth) would be given priority over LOCA when making financial safety investments.

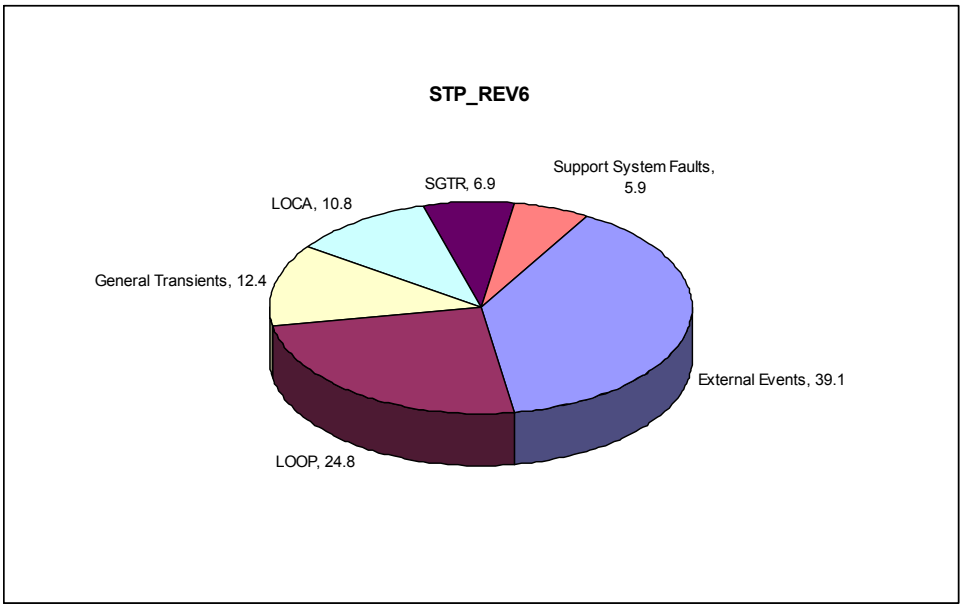

Figure 2. Percentage of total risk contribution at STP from dominant initiating accidents (from Rev 6 of STP site-wide PRA, Ref. 3).

Key uncertainties that currently dominate initial quantification of CDF and LERF contributions from recirculation include: (1) the size of the damage zone surrounding a pipe break (commonly referred to as the Zone of Influence, or ZOI), (2) the amount of debris that will pass through a STP strainer, and (3) the formation of chemical products in STP sump conditions (if any) and their degree of impact on head-loss at the strainer and within fuel assemblies. ZOI behavior is currently being investigated through a combination of computational fluid dynamics simulations and two-phase jet testing data obtained through participation in a Pressurized Water Reactor Owners Group (PWROG) collaboration. Rigorous strainer bypass testing using an STP prototype

strainer, and chemical formation and effects testing will be initiated and supervised by STP during the second project year.

Key conservatisms inherent to the initial quantification include: (1) very large assumed ZOI without benefit of truncation caused by concrete walls or directional limits imposed by whip restraints, (2) no credit taken for settling of fine debris in the containment pool before initiation of recirculation, (3) strainer bypass estimates based on a preliminary correlation of well-mixed pools containing excess fiber, (4) no credit taken for internal bypass of debris that passes through a fuel channel or travels around the core, (5) fuel channel deposition and performance challenges based on non-prototypic chemical debris types and unnecessarily high flow rates. A careful treatment of item #1 above could reduce maximum estimated debris volumes by a factor of 3.

Since the release of SRM SECY-10-0113, STP has engaged NRC staff in a series of prelicensing meetings to resolve questions about the methods employed for uncertainty propagation and risk quantification, and to elicit feedback on important analysis assumptions that may cause delays during formal review of a future licensing submittal. Important issues that have been identified to date include: (1) staff misgivings regarding STP interpretations and application of weld failure frequency data and associated expert elicitation reports, (2) staff admonishment regarding the proposed neglect of chemical effects in the initial quantification and precautionary advice given with respect to planned chemical formation and effects testing, and (3) a lack of strong consensus regarding the role of Regulatory Guide 1.174 in risk-informed resolution of GSI-191.

Weld rupture frequency data will be revisited early in project year 2 to examine an alternative implementation of expert opinion that is more familiar to the staff. Parametric studies of this type are transparently supported by CASA Grande. In response to very recent staff feedback, the initial quantification of CDF *does include* consideration of chemical effects for both strainer head-loss and in-vessel deposition concerns. Initial treatment is approximate, but is well grounded on limited available test data. Staff comments and concerns are being actively incorporated as STP-specific chemical effect test plans mature for project year 2. The final interpretation of RegGuide 1.174 and formal adoption of risk quantification for a new GSI-191

resolution strategy is still somewhat uncertain, however. Now that new tools and a competent team are available for rapid evaluation of residual concerns, it is recommended that the basis and flexibility of the risk-informed STP resolution strategy be reiterated to obtain high-level NRC endorsement.

No inherent difficulties have been identified with respect to the refinement and application of risk quantification methods developed for GSI-191 resolution. Additional information from testing and simulation will be essential for reducing dominant uncertainties, and additional refinement of both the STP PRA and CASA Grande will be needed to ensure a self-consistent treatment of time-dependent accident scenarios with multiple operator recovery actions; however, no theoretical impediments are known that will prevent maturation and successful academic defense of this methodology.

Supporting Analyses

The basic approach of this risk assessment is to automate the containment accident analysis so that plant performance metrics like head-loss across the sump strainers can be calculated for many thousands of postulated accident scenarios. The outcome of each scenario is properly weighted by the corresponding initiating event frequencies so that a distribution is formed containing both the magnitude of the accident consequences and also their relative likelihood of occurrence. In this case, the analysis comprises a sequential description of a LOCA accident sequence beginning with a coolant breach event and progressing through debris generation, transport, deposition, and bypass. All of the basic considerations included in a licensee response to GL 2004-02 (Ref. 4) must also be included in each risk-assessment accident sequence.

The primary analytic tools and assumptions used for the STP initial quantification are explained in this section including: (1) a basic description of information flow and statistical sampling in the risk evaluation process, (2) the sampling strategy used to obtain weld break size and probability weights, (3) compilation of uncertain failure probability, (4) strainer bypass correlation, and (5) chemical effects considerations.

Risk Evaluation Process and Assumptions

A multidisciplinary team was assembled to compile required information, build information interfaces, conduct simulations, exercise uncertainty quantification (UQ) strategies, and evaluate risk impacts in terms of CDF and LERF. Basic modules of the evaluation process are illustrated in Figure 3. For the initial quantification, several high-level assumptions were stated to define Year-1 scope:

(1) only welds are considered for pipe failure locations (through wall failure modes were judged to be at least 10 times less probable than weld failure mechanisms and can be added later as needed);
(2) time-dependence of debris formation, transport and arrival in combination with plant response is an essential aspect of the risk perspective;
(3) primary recirculation failure modes are sump-screen blockage exceeding limiting $NPSH_{margin}$ and fiber deposition in fuel assemblies, both with and without chemical effects (other modes such as air evolution will be examined in Year 2);

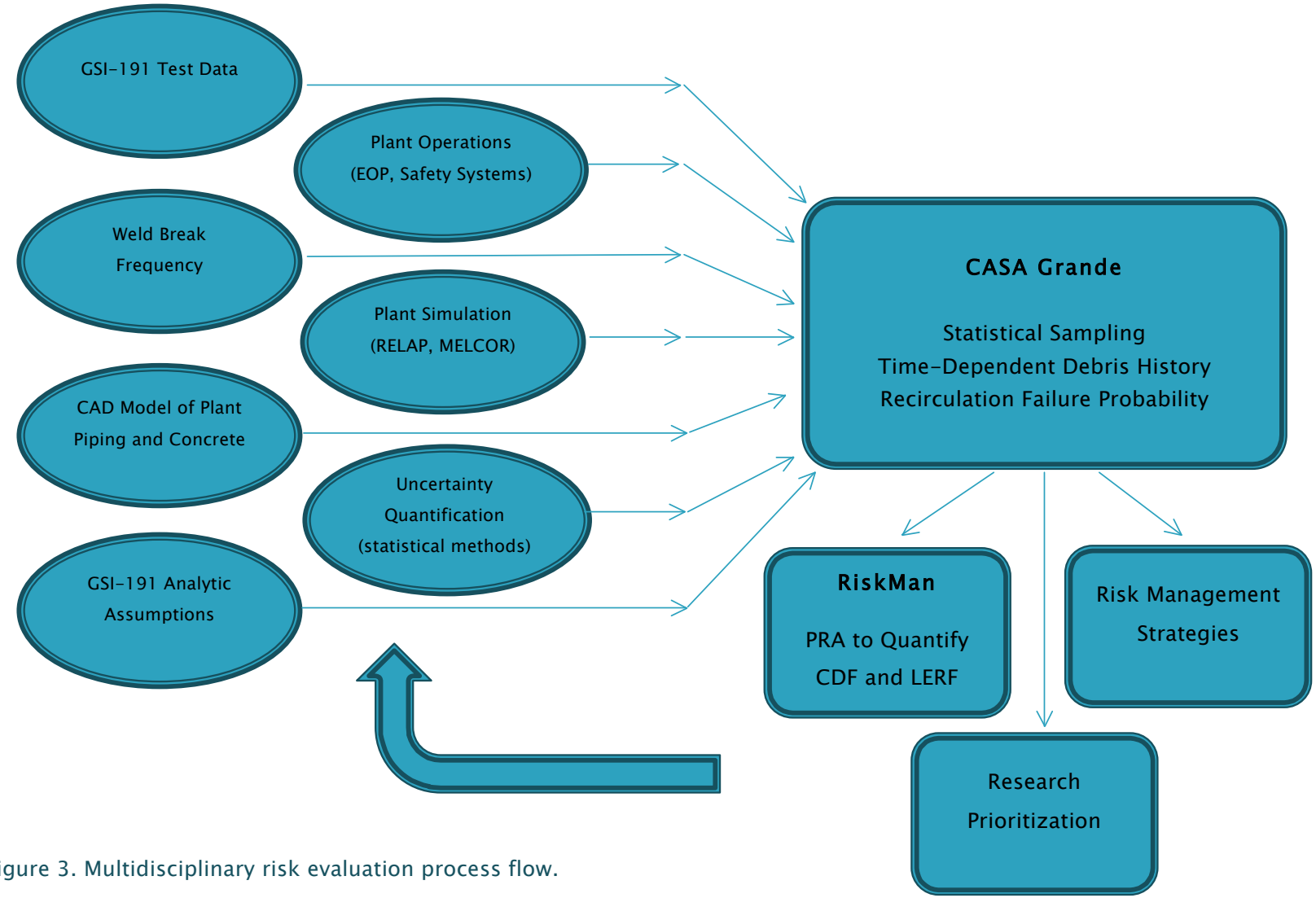

Figure 3. Multidisciplinary risk evaluation process flow.

(4) no credit for containment overpressure to simplify the interface with the PRA that includes scenarios with and without containment isolation;

(5) complete safety train failure (1, 2, or 3 trains fully operable) to simplify interface with the PRA that includes individual pump failure combinations (more complex scenarios will be examined in Year 2).

Automated calculation of debris volume for a spectrum of break scenarios relies heavily on CAD descriptions of the plant piping, insulation types and locations, and weld locations. The CAD data contains text labels for welds that are identified in the break frequency data as having unique attributes related to their composition, application method and inservice inspection history. When a break location and size is selected for analysis, physical coordinates are used to determine the damaged insulation targets in the vicinity of the break, exactly as it would occur in the plant.

An essential aspect of risk analysis is characterization of physical behavior over a full range of plausible conditions. Some aspects of GSI-191 have limited data support, and so uncertainty characterization is an important part of the description for each parameter. Specific examples include the size of the two-phase ZOI for Nukon™ fiberglass, and the proportion of fines vs. large pieces generated by the break. CASA Grande can process uncertainty distributions on any number of input parameters, but in the initial quantification, only the break frequency size distributions are permitted to have substantial ranges. Every other parameter is defined very close to commonly held regulatory assumptions to facilitate interpretation and communication of results.

Potential failure of the recirculation system to provide adequate cooling depends directly on the status of safety system components, and possibly the single most important metric for GSI-191 is flow rate. Flow rate across each sump strainer affects the amount and rate of debris accumulation and it determines the magnitude of pressure drop for water flowing through a debris bed. Similar considerations are true for debris deposition in fuel channels. Also, total flow rate through all available sump strainers determines the total rate and opportunity for bypass of fibrous material into the core.

Emergency Operating Procedures (EOP) were consulted to determine the operational timing of containment spray, low-head safety injection, and high-head safety injection pumps. Runout flow rates were assumed for all pump demands, and RELAP5 calculations (Section: Thermal-Hydraulics Analysis) that incorporate pump performance curves were used to understand the degree of conservatism in this assumption. One important finding from the operations staff is that containment spray is never initiated by a small break (< 2 in. equivalent diameter). Nominal times to drain the RWST and reach recirculation are presently used for each LOCA size category, but break-size specific times based on RELAP calculations may soon be interfaced to improve fidelity of the accident time histories. Similarly, MELCOR simulations may soon be available to provide break-specific containment pressure and pool temperature histories. Time-dependent water temperatures and corresponding NPSH histories are presently adopted from the STP final safety analysis report (Ref. 5)

The statistical method used for propagating uncertainties from numerous input parameters into distributions of head loss and fiber deposition per fuel channel is based on the mature and well-practiced theory of nonuniform Latin hypercube sampling (LHS). Reference 6 provides an academic presentation of the method with examples, but the basic description is straightforward:

(1) list the variables that are needed to completely specify one calculation of the physics model (complete list of input is often called a “vector”);
(2) form probability distributions over the range of every variable with significant uncertainty or physical variability (a uniform distribution between minimum and maximum limits expresses an equal probability of any value in the range);
(3) decide how many times the physics model can be evaluated in a practical amount of time (*N*);
(4) randomly select *N* values from the distribution of each parameter and determine the probability weight that each value carries (computed directly from the corresponding distribution);
(5) randomly combine the values of all parameters into *N* input vectors and form the product of weights for the parameters in each vector (random matching is sometimes called “sampling without replacement”);

(6) evaluate the simulation using each input vector and assign the multiplicative weight of the vector to each performance metric of interest as a probability of observing that outcome (a performance metric is simply the output of the calculation, x);
(7) rank order the N values calculated for the performance metric x and form the cumulative sum, $y(x)$, of successive probability weights in the ordered list;
(8) divide the cumulative sum by the total sum, Y, and plot $y(x)/Y$ vs. x to obtain a proper distribution of the output (read percentiles $\leq x$ directly from the plot);
(9) repeat as needed to obtain a stable estimate of any percentile of interest (repetition serves the important function of tracking convergence and quantify confidence).

Numerous variations exist on this basic protocol that improve the efficiency of the sampling for complex parameter spaces, avoid bias, and obtain faster convergence for the desired ranges of output. One of the most important features of the method for this application is the use of nonuniform probability weights for each parameter value. Nonuniform sampling enables efficient sampling of parameters with long tails, and this is important when the conditions of greatest interest lie at the extremes, like a double-ended guillotine break (DEGB) in the distribution of break size. Nonuniformity in the probability weights is introduced in Step 4, and a specific example is provided in Section: Sampling Strategy for Weld Brea. In the case of CASA Grande, evaluation of the physics models are comparatively fast, so 25 repetitions of ~3000 samples can be performed on a 64-bit, 2.3-GHz laptop with 6 GB of RAM in about 1 hour.

It is also important to note that nonuniform probability weighting is a fundamental technique used in most Monte Carlo solutions of complex physics and system dynamic problems in every branch of science. Examples of this approach can be found in radiation shielding, aerosol transport, financial market analysis, and transportation network simulation, to name only a few. The great power of nonuniform probability weighting lies in the ability to quantify conditions of interest that are extremely unlikely to occur on a purely random basis. Analog Monte Carlo techniques often employ adaptive variance reduction strategies such as “splitting” and “Russian roulette” to proliferate calculation scenarios in the desired improbable regions while terminating

those of little interest. In all methods, the total probability weight of all input parameters is conserved to avoid statistical bias.

Sampling Strategy for Weld Breaks

The first step in any LOCA sequence is to identify the location and size of the break. Reference 7 contains tabular distributions of break size frequencey for weld categories (called "cases") that are distinguished by commonality of metal composition, application method, structural purpose, inspection history, etc. An excerpt is provided in Table 1 for convenient reference. For each weld case (1B, 2, 3A, etc), the tables describe the annual exceedance frequency (# of events/reactor calendar yr) as a function of break size. The exceedance function simply reports the cumulative frequency of all events greater than or equal to a given size, *x*. For properly constructed probability distributions, the exceedance function is called a complementary cumulative distribution function (CCDF). Table 1illustrates the exceedance function for Weld Case 1B as a solid blue line and the corresponding columns in Table 1 show that the total frequency of all breaks in this weld case that are greater than 0.5 in. in size is 1.95×10^{-9} events/yr.

Reference 7 describes 45 separate weld cases. The sum of all exceedance frequencies greater than 0.5 in. is 3.815×10^{-4} breaks/yr. Starting with the excerpt in Table 1this is computed as $1.95\times10^{-9} + 1.98\times10^{-6} + 1.51\times10^{-7} + 1.51\times10^{-7} + \ldots$ Thus, the fraction of events in Case 1B, for example, is $1.95\times10^{-9}/3.815\times10^{-4} = 5.11\times10^{-6}$. A list of ratios like this for every weld case would describe the relative likelihood of experiencing breaks from each weld category *given* that a break of unknown size is assumed to occur. The example demonstrates the importance of knowing the total frequency of all breaks from all weld cases, because 3.815×10^{-4} events/yr represents the total initiating event frequency for all weld breaks considered in this study, and it must be distributed proportionally over all scenarios included in the statistical design.

Table 1. Example of annual break frequency distributions for several weld cases.

Calc. Case	1B		2		3A		3B	
System	Hot Leg		SG Inlet		Cold Leg		Cold Leg	
Size Case (in.)	29		29		27.5		31	
DEGB (in.)	41.01		41.01		38.89		43.84	
Weld Type	B-J		B-F		B-F		B-F	
DM	D&C		SC, D&C		SC, D&C		SC, D&C	
No. Welds	11		4		4		4	
	X, Break Size (in.)	**F(LOCA ≥X)**	**X, Break Size (in.)**	**F(LOCA ≥X)**	**X, Break Size (in.)**	**F(LOCA ≥X)**	**X, Break Size (in.)**	**F(LOCA ≥X)**
	0.50	1.95E-09	**0.50**	1.98E-06	**0.50**	1.51E-07	**0.50**	1.51E-07
	1.50	4.49E-10	**1.50**	4.59E-07	**1.50**	3.43E-08	**1.50**	3.43E-08
	2.00	3.36E-10	**2.00**	3.45E-07	**2.00**	2.38E-08	**2.00**	2.38E-08
	3.00	2.24E-10	**3.00**	2.31E-07	**3.00**	1.42E-08	**3.00**	1.42E-08
	4.00	1.55E-10	**4.00**	1.60E-07	**4.00**	9.49E-09	**4.00**	9.49E-09
	6.00	9.19E-11	**6.00**	9.52E-08	**6.00**	5.39E-09	**6.00**	5.39E-09
	6.75	7.83E-11	**6.75**	8.12E-08	**6.75**	4.53E-09	**6.75**	4.53E-09
	14.00	3.40E-11	**14.00**	3.35E-08	**14.00**	2.01E-09	**14.00**	2.01E-09
	20.00	1.80E-11	**20.00**	1.81E-08	**20.00**	1.15E-09	**20.00**	1.15E-09
	29.00	9.24E-12	**29.00**	9.57E-09	**27.50**	6.96E-10	**27.50**	6.96E-10
	31.50	7.97E-12	**31.50**	8.30E-09	**31.50**	5.63E-10	**31.50**	5.63E-10
	41.01	5.03E-12	**41.01**	5.24E-09	**38.89**	4.12E-10	**43.80**	3.38E-10

Excerpt from Ref. 7.

High-fidelity CAD data provide physical locations for all welds within each category, so collectively, the break frequency tables can be interpreted as a joint distribution of break size and break location. It is assumed that every pipe weld in a given category contributes an equal proportion of breaks at all sizes. For example, the 11 welds itemized for Case 1B each contribute $1.95\times10^{-9}/11$ events/yr of size $>$ 0.5 in., and they share identically shaped distributions of break size.

CASA Grande evaluates multiple sizes of breaks at *every* weld in containment, and it *always* includes the double-ended guillotine break (DEGB) condition for *every* weld. The total number of break scenarios investigated for each weld is determined by a user input parameter, Nbreak, that is arbitrarily set to 10 for the initial quantification. The range of break sizes for a given weld was subdivided into a number of intervals proportional to the range of the largest possible LLOCA. The standard LOCA bins of 0.5 to 2 in. (SLOCA), 2 to 6 in. (MLOCA) and $\geq$ 6 in. (LLOCA) are used for this study, although CASA can process any number of arbitrary LOCA bin definitions, so a uniform size interval (in.) is defined by the formula $\Delta S = \left(D_{\max} - 6\right)/\left(Nbreak - 1\right)$. The number of breaks per LOCA category is then determined by dividing the LOCA range by ΔS and rounding up to the nearest integer. Because the LLOCA range is much larger than the other two LOCA ranges, this process clusters a relatively large number of scenarios in the LLOCA category, which poses the greatest challenges to safety systems. Another important practical advantage to this algorithm is that no break-size intervals cross LOCA category boundaries.

Figure 4 illustrates the break-size selection process for Weld Case 1B, which includes the largest pipes in containment. LOCA category limits are marked with vertical solid lines. The DEGB condition, marked with a red dot, represents one of the 10 breaks imposed on the LLOCA range. The remaining 9 equal break-size intervals are separated by vertical dashed lines between 6 in. and 31.5 in. (the maximum pipe diameter). Note that the size intervals only appear unequal because of the logarithmic scale. By relative proportion of their respective ranges, only 2 break intervals are assigned to MLOCA, and only 1 is assigned SLOCA. Thus, 13 breaks are simulated at every weld belonging to Weld Case 1B. Using this process with Nbreak=10 generates 2843 break scenarios for every replication of the CASA analysis.

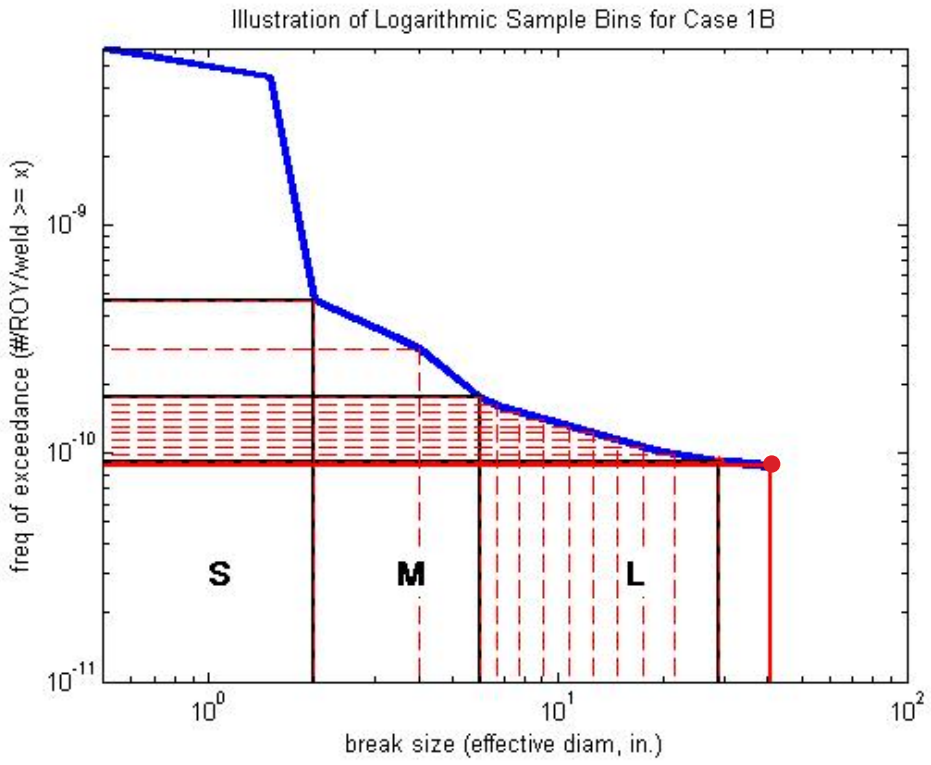

Figure 4. Example of nonuniform stratified sampling strategy for one 0077eld case that forces 10 samples for LLOCA (including DEGB), 2 samples from MLOCA and 1 sample from SLOCA.

A specific value of break size must be chosen from each of the defined intervals and corresponding probability weights must be assigned. This process is best explained by focusing attention on the vertical axis of Figure 4 and referring to Case 1B in Table 1. Example of annual break frequency distributions for several weld cases.. By subtracting cumulative values in the table, one finds that the total frequency of SLOCA from Weld Case 1B is $1.95\times10^{-9} - 3.36\times10^{-10} = 1.61\times10^{-9}$ events/yr. This value describes the range of break frequency above the highest horizontal line in Figure 4 (the upper boundary of the SLOCA category), and any single break from this range carries a probability weight of $1.61\times10^{-9}/3.815\times10^{-4}\ /11 = 3.84\times10^{-7}$. This is the proportion of all possible break frequency represented by one assumed break from this interval, and this weight is effectively assigned to the results of the scenario evaluation for any break selected from this interval. Logarithmic interpolation of the table ($\log_{10}$ by $\log_{10}$, consistent with Ref. 7) is used to determine annual exceedance frequencies at each of

the desired interval limits. Notice that the probability weights assigned to breaks selected from the LLOCA intervals are individually quite small, but the total probability (sum of all weights) is always conserved across the sample set.

The specific size of the break from each interval is chosen by the inverse process illustrated in Figure 5 for a SLOCA. First, a random number is chosen uniformly from the frequency range corresponding to the size interval of interest. Then, the distribution is "inverted" as shown by the green arrows in the figure. For tabular distribution functions, inversion is accomplished by linear interpolation within the table. For analytic distribution functions, inversion is accomplished through iterative numerical or analytic integration. The result of inverting the break-size distribution is one specific value of break size, chosen in a proportion consistent with the distribution function, that carries the probability weight of the local size interval. Random inversion is used to select specific break sizes from every size interval that is defined for all welds.

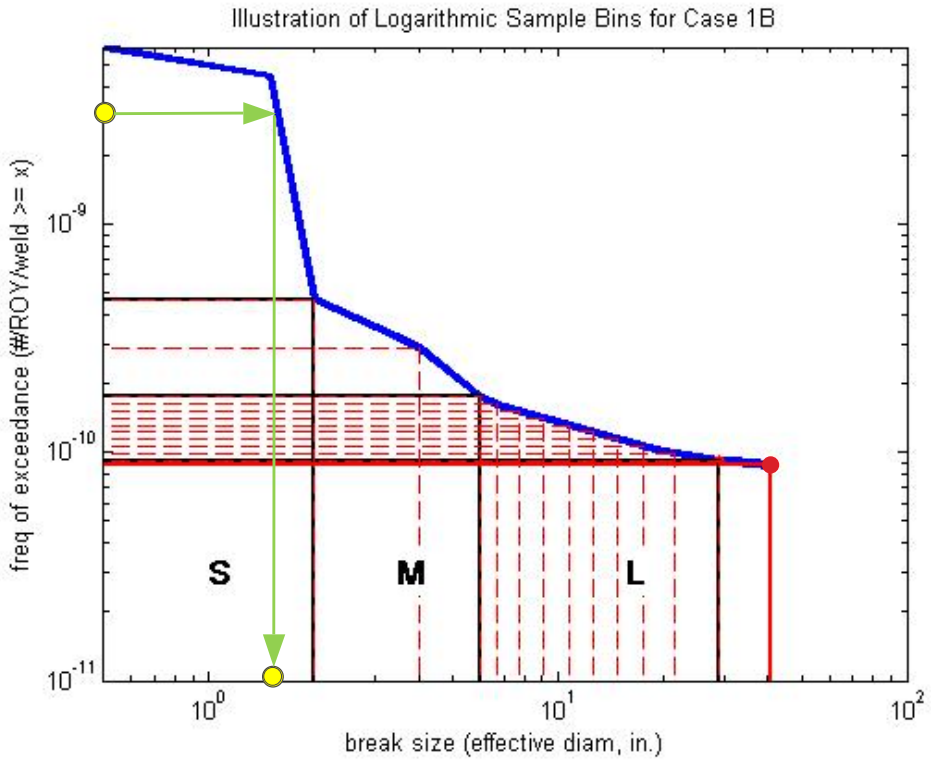

Figure 5. Illustration of inverse cumulative frequency sampling.

The DEGB condition is handled somewhat differently. Notice in Figure 5 that the last entry of any weld-case exceedance function (orange cell) defines the total annual frequency of the DEGB for that pipe, because there can't be any breaks larger than the DEGB. The corresponding size of 41.01 in. is actually a circular equivalent diameter that yields a total area equal to twice the severed pipe cross section. The second to the last entry provides the exceedance frequency of the actual pipe diameter. There is a debate in the fracture mechanics community suggesting that a linear weld rupture of a length equal to or greater than the pipe diameter will rapidly proceed to a full DEGB. Therefore, in CASA the pipe diameter exceedance frequency is always assigned to the DEGB condition. For Weld Case 1B, the pipe-diameter exceedance frequency is 7.97×10^{-12} events/yr and the corresponding probability weight for each DEGB event in Weld Case 1B is7.97×10^{-12} / $3.815\times10^{-4}/11 = 1.90\times10^{-9}$.

Several practical considerations deserve further mention:

(1) all break sizes are interpreted as circular equivalent diameters;
(2) any mismatch in weld counts between the frequency tables and the CAD data are scaled for consistency with the tables, because tabular initiating event frequencies are provided directly to the PRA;
(3) CASA reads an Excel™ spreadsheet of the format shown in Table 1. Example of annual break frequency distributions for several weld cases., any number of weld cases and any resolution of exceedance frequencies can be accommodated.
(4) Initial feedback from NRC staff has identified questions with the construction of break frequency exceedance functions like those shown in Table 1. CASA Grande can accept any generic tabular function for any number of weld types, so revision of the underlying break frequency assumptions does not pose a significant obstacle to rapidly regenerating the complete analysis.

Estimation of Failure Probability

A very useful definition of failure probability is simply: the fraction of observed cases that exceed a level of concern. Figure 6 illustrates the application of this definition for a continuous, analytic probability density function (PDF) of a generic performance measure. Given a sharp, well-defined decision threshold and a PDF with a total area of 1.0, the failure probability is found by integrating the area under the tail that exceeds the threshold. In CASA, an empirical approximation to the blue line is formed from a discrete number of scenarios, and in general, the performance distributions of interest have very long tails that imply very low failure probabilities. It is important to understand that the distribution of results from the accident simulations (blue line) embodies *all* of the physical variation in the space of possible scenarios. Causes of physical variation range from break size to water temperature, and include essentially everything that affects the outcome of a postulated accident. Random variations in every new batch of scenario descriptions cause fluctuations in the distribution of results (blue line), so independent estimates of failure probability relative to a sharp decision criterion will also vary. Every repetition of the analysis gives a slightly different answer, but the accuracy of the estimate improves with increasing number of replications. It is important to run enough cases to achieve an acceptable confidence level on the result.

Estimation of failure probability is somewhat more complicated when the threshold of concern also has an inherent uncertainty. A classic example of a threshold with considerable uncertainty is the amount of fiber that can be tolerated per fuel channel. Debris deposition in fuel channels is the latest issue to be associated with GSI-191, interpretation of recent data is ongoing, and legitimate questions can be posed regarding applicability of the test conditions to plant performance during an accident. These factors create additional variability in the estimation of recirculation failure caused by debris deposition in fuel assemblies that is not related to random physical behavior in the accident sequence.

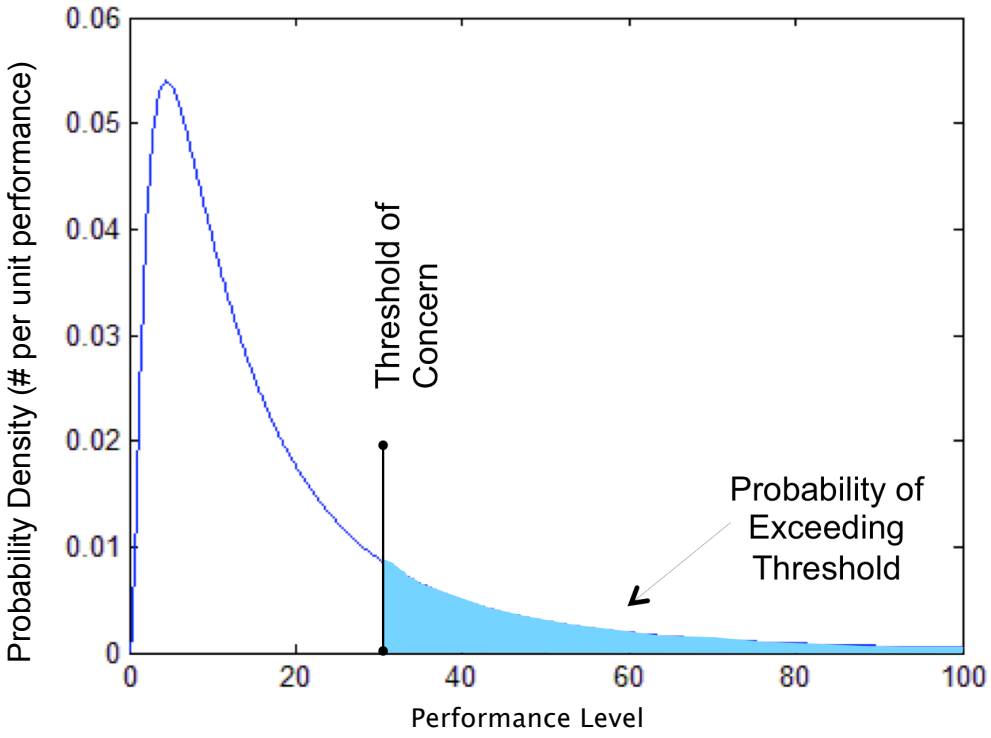

Figure 6. Definition of failure probability for a well-defined decision threshold.

Figure 7 illustrates the issue of calculating failure probability for a distribution of scenarios (blue line) when the fail/no fail criterion has width representing uncertainty (green line). For the purpose of illustration, both curves in the figure are smooth analytic density functions, but there is no practical reason why either or both functions cannot be tabulated using piecewise-continuous linear segments. This means that uncertainty in the tolerance level can be represented by any desired multifacet polynomial shape (triangle, rectangle, etc).

CASA treats decision-level uncertainty in exactly the same fashion as physical variability: every scenario in the LHS design is assigned a random failure threshold that represents an additional attribute of the accident. Similar to every other random parameter, the assigned failure thresholds also carry associated probability weights that represent their proportion of the tolerance uncertainty distribution (green line), so every scenario incurs one more multiplicative factor in its total probability weight that represents the successive combination of independent parameters. Final plant

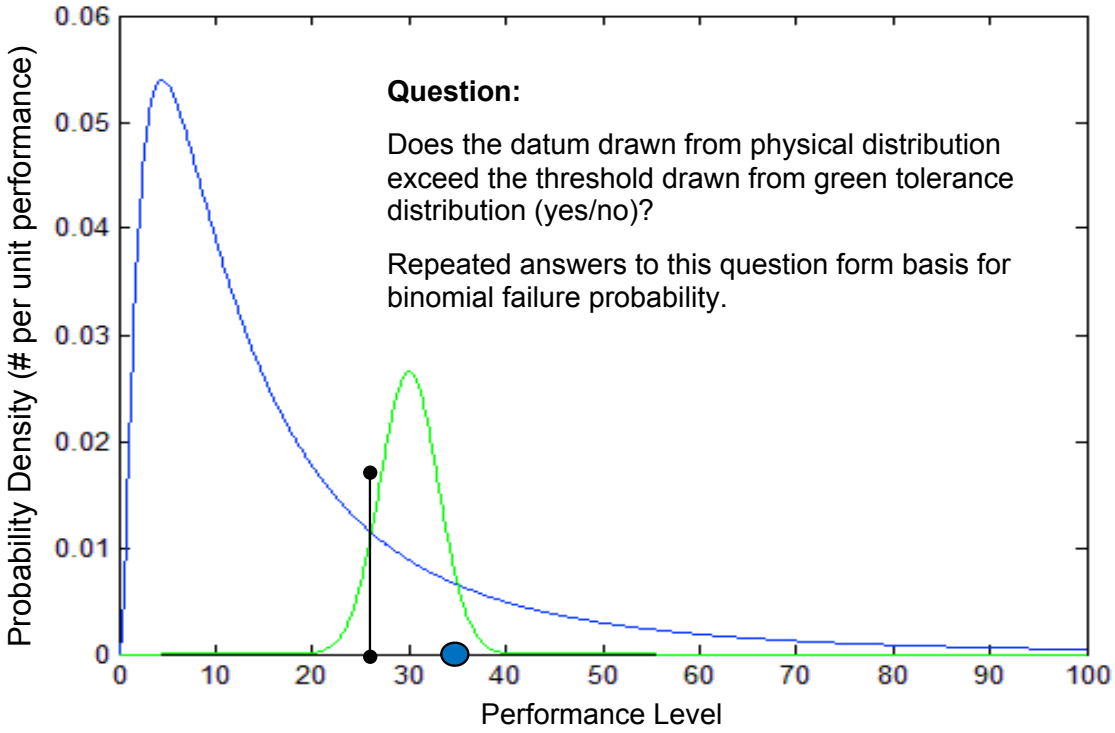

Figure 7. Estimation of failure probability with an uncertain decision threshold.

performance values (like mass of fiber per FA) are compared to their respective thresholds to build a binary list of fail/no fail (1/0) assessments for every scenario in the sample. The sum of scenario weights for cases that exceed their respective thresholds is divided by the sum of scenario weights for all cases to obtain the failure probability estimate. Separate failure probabilities for SLOCA, MLOCA and LLOCA are easily obtained by forming this comparative ratio of scenario weight for failed cases within the subpopulation of samples in each LOCA category.

A more sophisticated and less brute force method of folding decision-threshold uncertainty with performance metric distributions is being discussed for application in Year 2. This method involves postprocessing the two distributions outside of the LHS design by repeated application of the logic described for a sharp decision boundary. Each discrete decision level drawn from its uncertainty distribution carries a probability weight that can be used to form a distribution of values representing the

corresponding tail areas of the scenario distribution. Essentially, the process will build a probability distribution for the probability of failure. This method has the advantage of producing nonuniform confidence intervals on recirculation failure caused by various modes, and it will likely lead to stable estimates of mean failure probability using fewer CASA replicates.

Strainer Bypass Correlation

One of the more important parameters controlling the degree of fiber deposition in fuel assemblies is the amount of fiber that passes through the STP strainers. Limited data are available to characterize this phenomenon for the initial quantification in the range of flow velocity and pool concentration relevant for STP. With runout flow rates of containment spray, low-head injection and high-head injection pumps, the approach velocity across one sump strainer is estimated to be 0.009 ft/s when completely clean. For SLOCA and some MLOCA where the time to recirculation can be substantial, significant settling may occur in the pool, but tests are generally conducted with well-mixed pools containing excess quantities of fiber. Under these conditions, most of the fiber bypass occurs relatively quickly within a few pool turn-over periods while the strainer penetrations are largely unobstructed. As a fiber layer forms, the filtration efficiency improves and further bypass is minimized. For scenarios with insufficient volumes of fiber to form a contiguous mat, continued penetration of late-arrival debris types is possible.

Alion Science and Technology reviewed existing data to propose the correlation shown in Figure 8. Blue asterisks denote the 3 most relevant data points and the best-fit linear regression (with zero intercept) is shown as a solid central line with positive slope; 5^{th} and 95^{th} percentile confidence intervals on the slope are illustrated as dashed lines below and above the nominal fit, respectively. The proposed correlation of bypass fiber mass per 1000 ft^2 of strainer area depends only on the approach velocity, and hence, is insensitive to the size of the break or to the concentration of fiber in the pool. This may be a very reasonable description of bypass for conditions with excess fiber, because only a fraction of the total inventory must be collected in order to prevent penetration of the remainder. Additional data are needed to accurately characterize penetration for scenarios with much more dilute concentrations of suspended fiber.

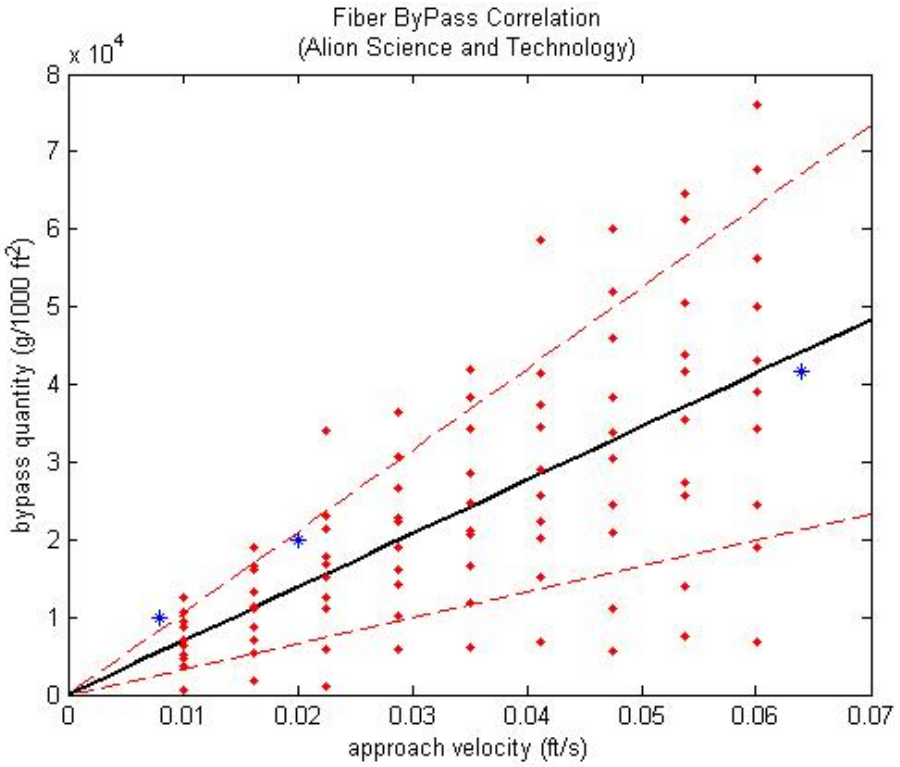

Figure 8. Fiber bypass correlation with approximate uncertainty bands.

Data used to develop the generic by-pass correlation were taken from the only three by-pass tests conducted at the time the correlation was developed. The strainers corresponding to the two lower approach velocities were Enercon "Top Hat" strainers and had a nominal hole size of 0.09" (2.3 mm). The strainer for the highest approach velocity was a PCI small-scale circular stacked disk strainer with a nominal hole size of 1/8" (0.125" - 3.17mm). STP uses the PCI SureFlow™ design with a nominal hole size of 0.095" (2.4mm). The fiber used in all tests was mechanically shredded NUKON™ with a size distribution characteristic of NUREG/CR-6224 Classes 1 through 3 (Ref. 8) in conformance with the March 2008 NRC head loss testing guidance. The fiber was boiled for 5 minutes and rinsed with tap water. The boiled fiber was diluted in a 5 gallon bucket and added in 1/8th inch equivalent bed thickness batches until all the surface area of the strainer was covered. The by-pass debris was captured by a 5-micron 100% flow filter bag.

Significant uncertainties envelope a linear regression based on only 3 data points, but there is at least one datum in the proper range to describe STP flow conditions. Note that the spread of the confidence bands increases with increasing approach velocity, so the uncertainty distribution on bypass mass must be evaluated for any required flow rate and surface area that develops during a time-dependent accident scenario. For expediency, the 5th percentile, mean and 95th percentile were used to determine the standard deviation of a corresponding normal probability distribution for any required velocity[1]. The normal distribution was then sampled to return random penetration quantities (and probability weights) as needed for the statistical design. For illustration purposes, red dots in Figure 8 mark random samples taken from these distributions as a function of approach velocity. A hybrid variation of the LHS design was employed whereby *all* of the LHS event scenarios *each* received 10 values of fiber bypass rather than the single matching of values used for other parameters. This approach emulates the strategy of "splitting" used in analog Monte Carlo solutions of physical process to refine estimates of unlikely parameter combinations. In this case, added resolution in the description of bypass uncertainty improves the stability of recirculation failure probability with fewer CASA replications.

Wide uncertainty bands on the bypass quantity can lead to predicted values that exceed the total inventory of latent plus damage-induced fiber that is present in a scenario. A logic check was implemented in CASA Grande to prevent more than 100% fiber bypass. This is the only direct influence of break size that is imposed on the bypass correlation.

Chemical Effects Considerations

Chemical effects can impact both strainer blockage and core blockage. The following discussion provides the method and basis used to incorporate chemical effects in the initial CASA Grande quantification.

[1] Uncertainty on a regression slope with only 3 data points should actually be distributed as a Student's t distribution rather than as a fully developed normal distribution. All continuous distributions are truncated and renormalized to desired limits to ensure positivity, etc.

Strainer Blockage

For cases where the strainer is not fully covered with fiber debris, chemical precipitates can pass directly through the strainer without any significant impact on head loss. A 1/8th inch equivalent fiber bed on all operating strainers is assumed to provide full coverage.

STP has plant-specific strainer test data showing that following the addition of chemical debris (prepared per the requirements in WCAP-16530-NP (Ref. 9)), the head loss approximately doubled. The fiber loads for this test were based on a 31-inch double ended guillotine break with a 7-D radius ZOI. The precipitate quantities were calculated using the WCAP spreadsheet. The inputs used for the WCAP calculation were strongly biased in a manner that significantly increased the quantity of precipitates compared to calculations based on more realistic inputs.

For the initial quantification, no bump-up factor was included for chemical effects in cases where the strainer is not fully covered with fiber debris. In cases where the strainer is fully covered, the calculated head loss was doubled to account for chemical effects. However, since chemical precipitation is not expected to occur until later in the event, the chemical effects bump-up was only applied for head loss values after 24 hours.

In-core Blockage

Within the core, the potential for blockage is largely dependent on the break location, injection location, and timing. The following time-dependent processes are important considerations for in-core blockage:

- At STP, the SI flow from all three ECCS trains is initially injected in the cold legs. Between 5.5 hours and 6.5 hours after the initiation of recirculation, two trains are switched over to hot-leg injection and one train is left on cold-leg injection (Ref. POP-05).
- Fine debris that is blown or washed to the pool prior to the start of recirculation would transport to the strainers within 5 pool turnovers (approximately 3 hours). Therefore, the majority of the fiber debris bypass would likely occur

during cold-leg injection. However, longer term debris arrival at the strainer could occur due to

- Fines gradually eroded from non-transporting pieces of fiberglass
- Delayed washdown of fine debris later in the event
- Failure of unqualified coatings later in the event
- Chemical precipitation later in the event
- Debris captured in the core during cold-leg injection and subsequently back-flushed out of the core upon switchover to hot-leg injection

If the strainer is fully covered with a fiber bed, most debris (especially fibrous debris) would be captured in the debris bed and would not bypass the strainer. However, based on preliminary results from CASA Grande, the vast majority of break cases would not generate enough fiber to fully cover the strainers at STP. Therefore, long term bypass during hot-leg injection is a potential concern.

- Due to the time required for physical processes related to chemical effects to occur (corrosion/dissolution of containment materials, reduction in pool temperature, kinetics of precipitate formation, etc.) significant chemical precipitation is not expected to occur for at least 24 hours. Therefore, chemical effects would not be a significant factor during cold-leg injection.
- The flow rate required to remove decay heat from the core will steadily decline as shown in Figure 9. The required flow rate at various points in time are:
  - 0.3 hr (start of recirculation): 634 gpm
  - 6 hr (switchover to hot-leg injection): 261 gpm
  - 24 hr: 167 gpm
  - 720 hr (end of mission time): 46 gpm

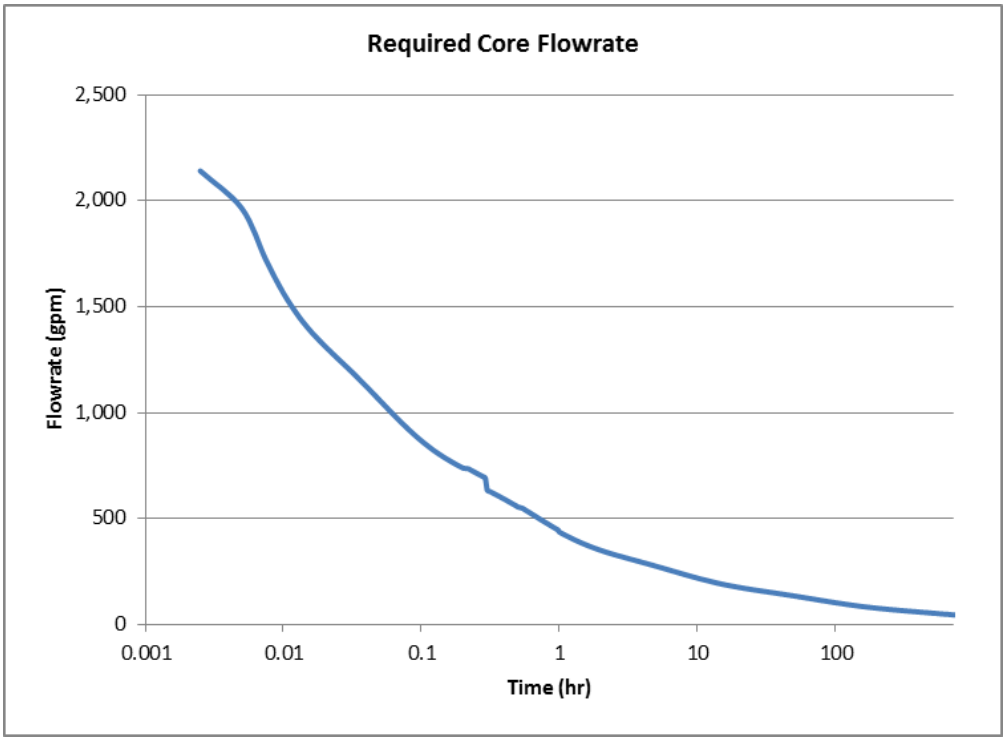

Figure 9. Flow rate required to remove decay heat.

The following figures and discussion illustrate the flow paths and potential core blockage corresponding to 1) cold-leg injection for a cold-leg break, 2) hot-leg injection for a cold-leg break, 3) cold-leg injection for a hot-leg break, and 4) hot-leg injection for a hot-leg break. This discussion is based on large break conditions. However, these conditions are generally equivalent or bounding for smaller break sizes.

Large Cold-Leg Break

Figure 10 and Figure 11 illustrate the flow paths for a break on the cold-leg side during initial cold-leg injection and long term hot-leg injection respectively. During cold-leg injection, the minimum flow required through the core to remove decay heat would be limited to the flow required to replenish boil off. The driving head would be the difference in the elevation of the water level in the cold leg (or the elevation of the break if it is above the cold leg) and the water level above the core. The elevation of the bottom of the cold leg is 31.1 ft and the elevation of the top of the active fuel is 26.9 ft. Therefore, the minimum acceptance criteria for this scenario would be a head loss within the core of 4.2 ft. The debris that bypasses the strainer would initially be split between the SI and CS flow. The debris transporting with the SI flow to the reactor vessel would then be split again with a small fraction transported to the core and the remainder transported back out to the pool through the break. The flow required through the core just to remove decay heat would vary from approximately 630 gpm (3.3 gpm/FA) at the beginning of recirculation to 260 gpm (1.3 gpm/FA) at switchover to hot-leg injection. The total SI flow would vary from 4,420 gpm for one train operation to 13,260 gpm for three-train operation. Therefore, the flow split (and debris transport) required to the core would be approximately 14% for single train operation and 5% for three train operation (assuming the strainer bypass occurs right at the start of recirculation). Since chemical effects would not be a factor during cold-leg injection, the test cases that are most applicable to this scenario are [ ][2]. [ ] Since this head loss is less than the acceptance criteria of 4.2 ft, 75 g/FA is an acceptable fiber load for a cold-leg break during cold-leg injection. Note that 75 g/FA in the core is equivalent to over 500 g/FA within the reactor vessel since 85% to 95% of the debris would bypass the core in this scenario. However, bypass within the core is conservatively *not* credited in the initial CASA analysis.

[2] Bracketed text represents proprietary data taken from WCAP-17057-P, "GSI-191 Fuel Assembly Test Report for PWROG", Revision 1, September 2011.

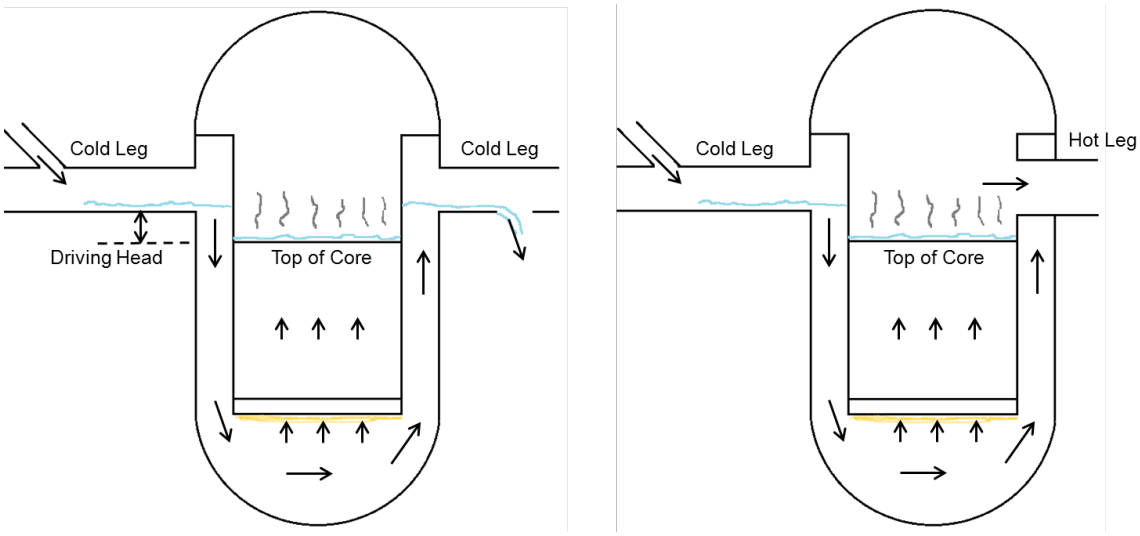

Figure 10. Cold-leg injection for a cold-leg break.

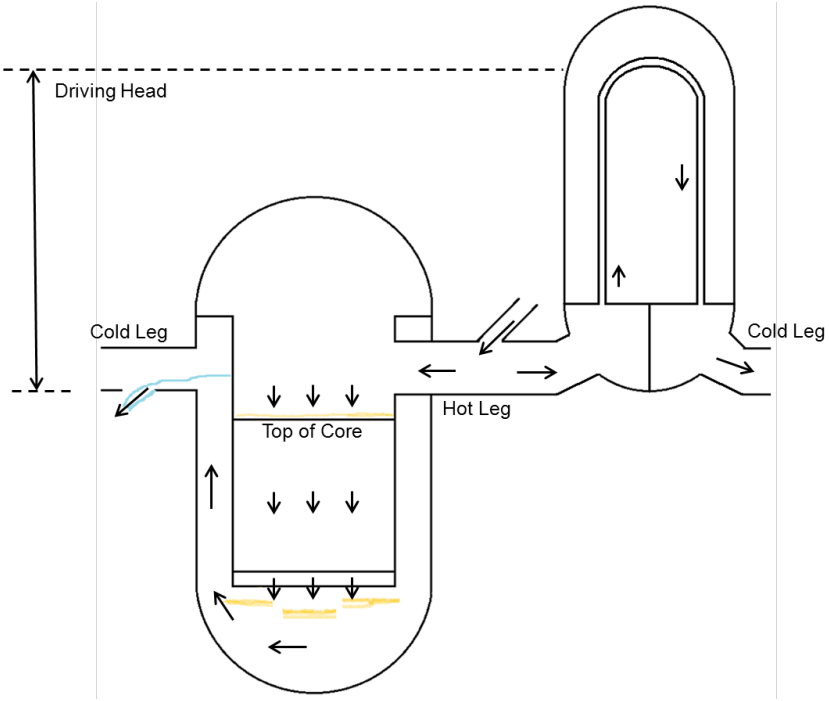

Figure 11. Hot-leg injection for a cold-leg break

Approximately 5.4 hours after the start of recirculation, two SI trains would be switched over to hot-leg injection with approximately 8,840 gpm flow through the core. The debris that accumulated in the core during cold-leg injection would tend to be backflushed out of the core as shown in Figure 11. Fiber, particulate, and chemical precipitate debris may bypass the strainer during hot-leg injection and could accumulate in the core. If this happens, the head loss would raise the water level in the steam generator tubes until it spills over the tubes and bypasses the core by exiting the break from the opposite side[3]. The elevation of the steam generator tube spillover point is 72.3 ft and the elevation of the bottom of the cold leg is 31.1 ft. Therefore, the minimum acceptance criteria for this scenario would be a head loss within the core of 41.2 ft. Since head loss is proportional to the flow rate, the reduced flow would allow for the accumulation of additional debris in the core. The flow rate required for decay heat removal during hot-leg injection would range from approximately 260 gpm (1.3 gpm/FA) at the beginning of hot-leg injection to 50 gpm (0.3 gpm/FA) at the end of the mission time. It is assumed that an actual flow rate of 580 gpm (3.0 gpm/FA) through the core would be sufficient to prevent boron precipitation. It is also assumed that the head losses within the core would be essentially the same for the hot-leg injection flow path as for the cold-leg injection flow path given an equivalent debris load and flow rate (i.e. debris accumulation with flow from the top to the bottom of the core would have essentially the same head loss as debris accumulation with flow from the bottom to the top of the core). Therefore, the cold-leg injection tests in WCAP-17057-P are assumed to be applicable to hot-leg injection as well. The test cases that are most applicable to this scenario are [ ]. [ ]

[3] A potential concern is that once water starts to spill over the steam generator tubes, a siphon effect may occur that would draw all of the water out of the reactor vessel. However, since a siphon doesn't work if the pressure drops below the vapor pressure of the fluid, the tallest siphon possible is approximately 33 ft under standard pressure and temperature conditions. At elevated temperatures, the maximum siphon height is much lower.

[redacted] Since this head loss is less than the acceptance criteria of 41.2 ft, 75 g/FA is an acceptable fiber load for a cold-leg break during hot-leg injection.

Large Hot-Leg Break

Figure 12 and Figure 13 illustrate the flow paths for a break on the hot-leg side during initial cold-leg injection and long term hot-leg injection respectively. During cold-leg injection, the full SI flow (up to 13,260 gpm for three train operation) would pass through the core, and any fiber and particulate debris that bypasses the strainer could accumulate in the core. If this happens, the head loss would raise the water level in the steam generator tubes until it spills over the tubes and bypasses the core by exiting the break from the opposite side. The elevation of the steam generator tube spillover point is 72.3 ft and the elevation of the top of the active fuel is 26.9 ft. Therefore, the minimum acceptance criteria for this scenario would be a head loss within the core of 45.4 ft. Since head loss is proportional to the flow rate, the reduced flow would allow for the accumulation of additional debris in the core. The flow rate required for decay heat removal during hot-leg injection would vary from approximately 630 gpm (3.3 gpm/FA) at the beginning of recirculation to 260 gpm (1.3 gpm/FA) at switchover to hot-leg injection. Since boron precipitation is not a concern during cold-leg injection, it is not necessary to exceed the flow rate required for decay heat removal. As discussed previously, chemical effects would not be a factor during cold-leg injection. [redacted] The maximum head loss in all of these tests prior to the addition of chemical precipitates was below the acceptance criteria of 45.4 ft. Therefore, 150 g/FA is an acceptable fiber load for a hot-leg break during cold-leg injection.

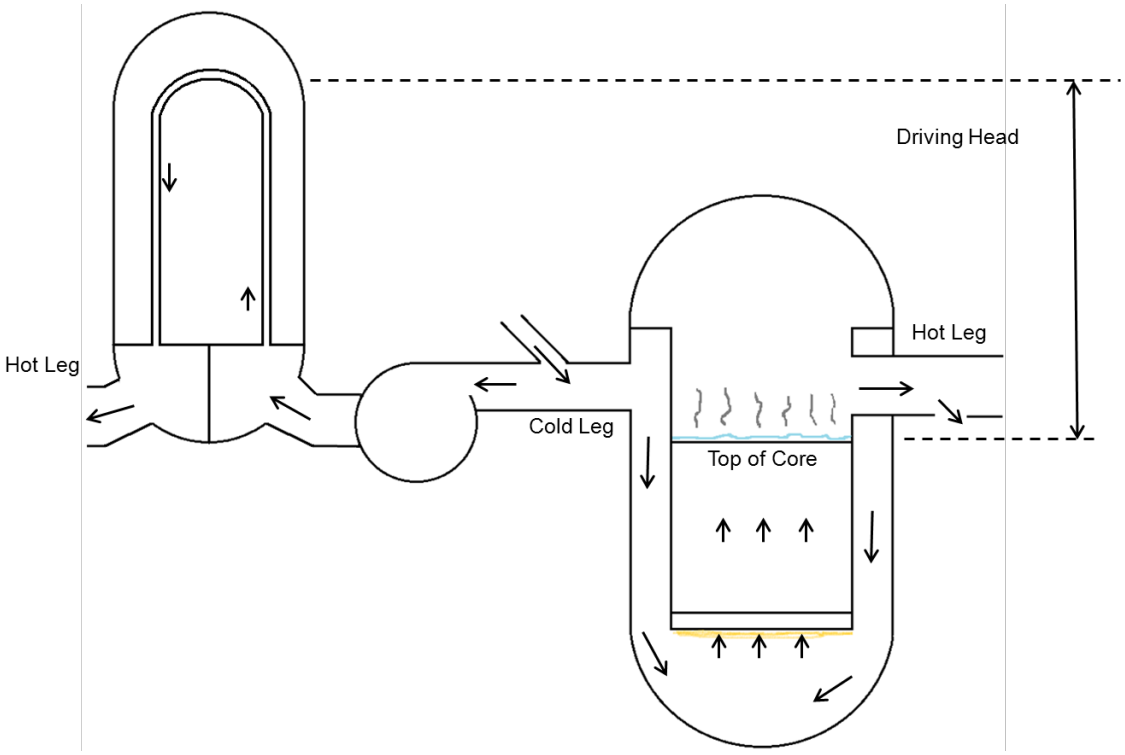

Figure 12. Cold-leg injection for a hot-leg break

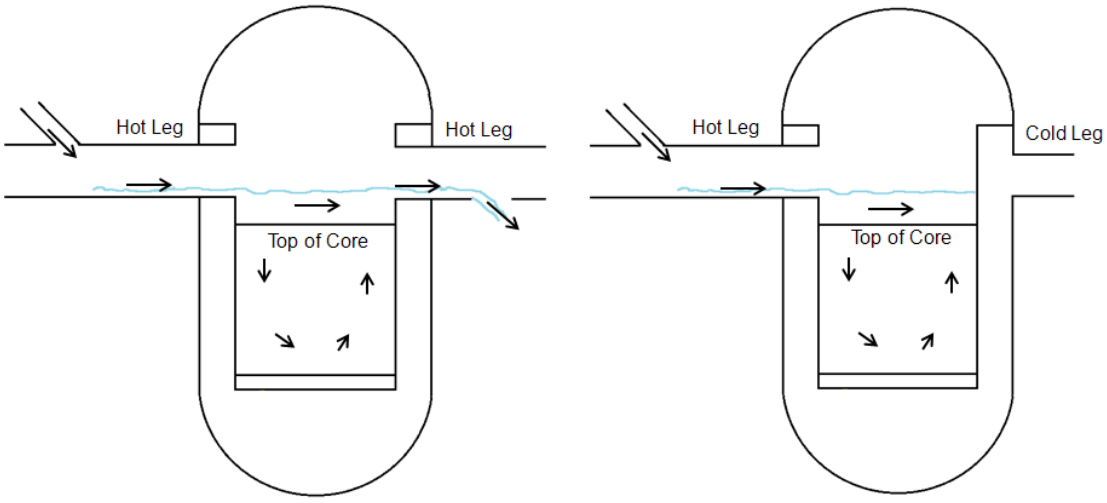

Figure 13. Hot-leg Injection for a hot-leg break

Approximately 5.4 hours after the start of recirculation, two SI trains would be switched over to hot-leg injection. The flow would pass directly from the hot-leg injection locations, over the top of the core, and out the break as shown in Figure 13. Fiber, particulate, and chemical precipitate debris may bypass the strainer during hot-leg injection, but there are no locations where significant core blockage would occur in this scenario. Therefore, strainer debris bypass is not a concern.

Chemical Effects Summary

Table 2 summarizes the method used to incorporate chemical effects within the initial quantification. Core damage is assumed to occur for any cases that exceed the acceptance criteria.

Table 2. Summary of method used to incorporate chemical effects in initial quantification for STP.

Scenario	Chemical Effects Bump-Up Factor	Acceptance Criteria
<1/8" fiber bed on active strainer(s)	1.0	time dependent head loss < time dependent NPSH margin
>1/8" fiber bed on active strainer(s)	2.0 (after 24 hours)	
Cold-leg break/cold-leg injection	N/A	>500 g fiber per FA
Cold-leg break/hot-leg injection	N/A	75 g fiber per FA
Hot-leg break/cold-leg injection	N/A	150 g fiber per FA
Hot-leg break/hot-leg injection	N/A	>>150 g fiber per FA

Based on this evaluation for STP, a fiber bypass quantity of 75 g/FA is acceptable for all breaks on the cold-leg side, and a fiber bypass quantity of 150 g/FA is acceptable for all breaks on the hot-leg side. Although it can easily be added, the current input in CASA Grande does not specify whether a break is on the cold or hot-leg side. For the initial quantification, an equal probability was assumed for breaks on either side. To do

this, CASA Grande was run using the 75 g/FA acceptance criterion and rerun using the 150 g/FA acceptance criterion. The results from these two runs were averaged together to determine the recirculation failure probability that was passed to the PRA for estimation of core damage frequency. Failure probabilities separately averaged over small, medium, and large break sizes were developed.

CASA Grande

The Containment Accident Stochastic Analysis (CASA) tool was developed to facilitate risk-informed resolution of GSI-191 by automating the methods commonly used to analyze LOCA-generated debris formation, transport and accumulation and by providing a framework for statistical uncertainty propagation. The word "stochastic" refers to both the random variability inherent in many of the accident phenomena *and* the random sampling methods used to propagate parameter uncertainties into distributions of safety system performance metrics such as suction strainer head loss and debris bypass. Among the insights gained from CASA are recirculation failure probabilities to populate branch fractions in site-wide PRA scenarios that involve varying numbers of operable sump trains and containment spray conditions, but additional opportunities for parametric sensitivity studies, risk management, and research prioritization are fertile. This section first provides a general overview of CASA to describe basic functional elements like input requirements and analysis flexibility. Then, a brief technical discussion is provided to document the treatment of time-dependent debris concentrations. Finally, examples of typical output are provided as generated for the STP initial quantification.

General Description

As suggested earlier in Figure 3, CASA serves as an integration platform for collecting the body of knowledge gained from over 10 years of research in GSI-191 phenomenology and rapidly analyzing thousands of accident scenarios to form probability distributions for important decision metrics related to plant operability under recirculation conditions. CASA emphasizes three attributes of containment accident analysis that are essential for building a complete and accurate risk perspective; these fundamental attributes are (1) time-dependent interaction between debris arrival and the plant safety systems, (2) relative occurrence frequency for the

spectrum of LOCA initiating events, and (3) realistic distributions of parameter variability that capture the relative proportion of values across the range of concern.

CASA was developed with 4 primary software objectives:

(1) flexibly accommodate any number of random variables (parameters) with the ability to accurately quantify the influence of extreme conditions like DEGB frequency;
(2) accept totally external input definitions so that there are no embedded data;
(3) support uncertainty propagation through inherently time-dependent physical processes;
(4) modular treatment of data processing so that future variations in format and information content can be incorporated easily.

Given the relatively short development time available for the initial quantification, the present version of CASA satisfies all 4 objectives to a large degree. Although the present version could be exercised successfully by a user knowledgeable in the MatLab™ programming language, the package is not yet sufficiently mature to warrant a graphic user interface or a beta-test users group.

Required input to CASA includes plant geometry for (1) pipes, (2) welds (3) tanks and equipment, (4) pipe restraints, and (5) insulation applied to any of the above. These data can be derived from existing CAD models or directly from drawings. As noted, the CASA data interface can be modified to accept alternative formats. To facilitate plant geometry definition for STP, Alion Science and Technology developed a data extraction utility that pulls essential coordinates out of an existing CAD model built in AutoDesk Inventor™. CASA reads formatted text files and reconstructs piping runs with insulation applied. To identify both targets and point of origin, text labels in the data identify insulation types and weld case associations. These spatial data are critical for calculating the realistic range of debris volume and composition that can be generated by the population of assumed breaks.

Figure 14 provides sample graphics from CASA illustrating how spherical ZOI might intersect insulated pipes and large equipment. In CASA, the insulation has been discretized into small volume elements for convenient integration within the ZOI.

Spherical ZOI are only applied for DEGB cases; all other breaks are assumed to have hemispherical ZOI randomly directed perpendicular to the pipe wall where the break occurs.

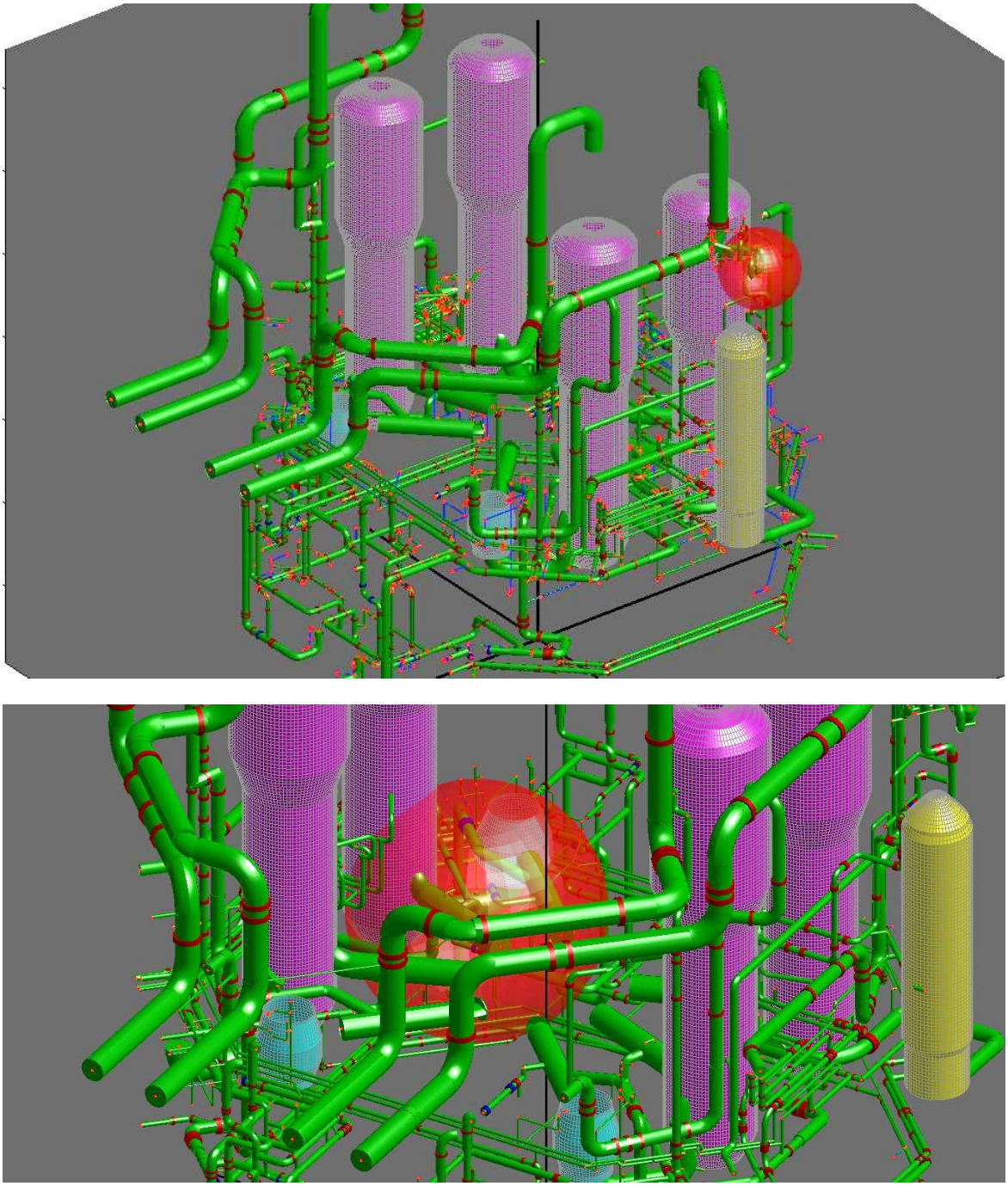

Figure 14. Sample graphics from CASA Grande of ZOI (red spheres) intersecting STP pipes and equipment.

Concrete barriers and gratings are presently ignored by CASA, but they can be specified in STL graphics format and imported for visualization. Truncation of ZOI geometries by solid boundaries is a refinement that will be added early in Year 2. Algorithms for intersection of spherical ZOI have already been formulated. Spatial data defining the location and surroundings of the break relative to gratings may also provide a defensible basis for retention factors in future versions.

In addition to the plant geometry, CASA requires full specification of LOCA frequencies as a function of pipe break size. Again, formats can be altered to accept varying degrees of resolution in the available information. LOCA frequencies by size are used to define conditional probabilities that are properly sampled to propagate entire distributions of scenarios (as described in Section: Sampling Strategy for Weld Breaks). CASA currently assumes that break frequency distributions are provided in a CCDF (or exceedance function) format in time rate units of breaks/yr/weld. Because the break frequency data for SLOCA, MLOCA and LLOCA may be provided independently to a PRA, CASA always preserves the normalization of the table and treats the CAD weld population as a representation that introduces spatial granularity.

Any number of weld cases (type or category) can be provided with varying resolution, but the last entry in each curve is interpreted as the effective DEGB size and the next to the last entry is interpreted as the inside diameter of the pipe class in question. By convention, the DEGB size is calculated as the diameter of a circular area equal to twice the cross sectional area of the pipe so that $D_{DEGB} = \sqrt{2} D_{pipe}$. The DEGB size is not used explicitly anywhere in the calculation, nor is the associated DEGB exceedance frequency. As explained earlier, it is assumed that circumferential tears longer than the pipe diameter rapidly proceed to full separation, so the larger exceedance frequency reported for the actual pipe diameter is assigned to the DEGB condition. Similarly, spherical ZOI radii for DEGBs is also based on the inside pipe diameter.

Total plant-wide break frequency for any given weld case is obtained by multiplying the per weld distributions by the number of welds assumed in each weld case (see Table 1). Independently developed CAD data may contain a somewhat different weld count for each category. Where discrepancies are noted between the number of welds per case in the CAD and the number of welds per case in the tables, the CAD available

locations are scaled to carry a probability weight consistent with the table. Warnings are generated when probability scaling occurs. It is important to maintain consistency with the tables, because these initiating event frequencies are also provided directly to the PRA.

If any weld cases in the frequency tables have nonzero assumed weld counts, but no corresponding weld locations appear in the CAD, the SLOCA, MLOCA, LLOCA break frequency for those cases is separately redistributed across all other weld cases that do have CAD representations in proportion to their relative break potential. Redistribution has the effect of mapping weld cases that are missing from the CAD model onto other piping runs to approximate the spatial distribution of breaks associated with the missing cases. Break frequency redistributed from missing weld cases to existing weld cases is added to the upper size limit of each respective LOCA category in the recipient cases. Assignment of redistributed break frequency to the upper limit of each LOCA category has the effect of inflating the frequency of all break sizes within the category.

Repeated iteration between the STP CAD model and the weld case definition file has significantly improved the consistency and completeness of weld labels. Only a few minor discrepancies remain between the CAD model and the frequency tables that require probability scaling to compensate for differing weld counts. There are no weld cases missing from the CAD model that require break frequency redistribution.

Distributions of break size provided by weld type are generally provided as exceedance functions (complementary cumulative) in units of breaks per year per weld. The sum of total frequency over all weld cases yields the plant-wide total frequency of weld breaks per year of all sizes. The easiest way to interpret subdivision of these distributions into LOCA size categories, and then further into nonuniform sample weights, is to simply think in terms of the incremental break frequency contribution from each subdivision. The conditional probability of any subdivision is then just the ratio of incremental frequency for the condition of interest to the plant-wide total frequency.

In general, the break frequency table should be interpreted as a joint distribution of break size and break location. With this point of view, the weld case columns are related to complementary conditional probabilities, or slices of the joint distribution. Break location is not a smooth continuous random variable in the traditional sense. In

this application, break frequency in each weld case column is mapped to discrete spatial coordinates through geometry descriptions in the CAD model. Nonetheless, the analogy to a bivariate joint distribution function is sound.

CASA imposes the assumption that any equivalent break size equal to or larger than the nominal pipe diameter will rapidly proceed to a DEGB. To enforce this assumption, the cumulative exceedance frequency in each weld case distribution of breaks larger than the nominal pipe diameter is applied to the DEGB. For break-size distributions, it is always assumed that larger breaks lead to larger consequences. For other random variables, the user may specify either the lower or upper tail to be the conservative range.

Break frequency data has been extrapolated to an effective diameter of $\sqrt{2}D_{pipe}$ to account for double-sided break area. This extrapolation is not actually needed, because ZOI geometry is based only on D_{pipe}. When $D_{break} < D_{pipe}$, the ZOI is modeled as a hemisphere directed perpendicularly away from the pipe with a random azimuth and a radius R_{ZOI} scaled to the damage distance of each insulation type. When $D_{break} = D_{pipe}$, the event proceeds to a DEGB and the ZOI is modeled as a full sphere with the same ZOI damage radii. Thus, for an insulation type with a damage potential of (radius/diameter) R/D = 17, the presumed spherical ZOI radius is set equal to 17D.

CASA uses a nonuniform LHS sampling routine that guarantees the DEGB conditions are included in every replicate batch. This is possible by treating each DEGB as a degenerate size bin having zero width but finite probability weight (delta function). Each parameter that is accessible as a random variable can have a different probability distribution defined on linear or logarithmic ranges. Sampling of each distribution may vary in the degree of logarithmic expansion (explained below), and they may have different definitions of conservative direction across their range. The present routine builds a non-optimized LHS design based on combining without replacement random values taken from nonuniform bins defined on each variable range (see Section: Sampling Strategy for Weld Breaks).

Logarithmic expansion of a probability range for the purposes of nonuniform stratified sampling of a random variable is a generalization of a concept illustrated in Figure 5

that presents break-size exceedance frequency on logarithmic scales in base 10. The logarithmic scale emphasizes fine details in the remote upper tail of the distribution function by "expanding" resolution in the probability range by successive factors of 10. If logarithmically equal intervals are selected along the range of the $\log_{10}$ ordinate (nonuniform probability bins on a linear scale), a predominance of samples will be extracted from the upper tail of the distribution. Sampling values from uniform bins on a linear scale would almost never select the extreme tails (less than 1 in a million samples, for example). Logarithmic expansion in base 2 would provide successive doubling of the resolution and fewer samples than base 10 would be preferentially selected from the upper tail. Logarithmic expansion in base 42, etc. would lead to even more interrogation of the upper tail than base 10. Thus, choice of the logarithmic base can be used to control the degree of expansion over the range of the variable. Note that the logarithmic scale of the x axis in Figure 5 is for presentation clarity only and has nothing to do with the strategy of logarithmic expansion.

If exactly the same logarithmic expansion scheme is used to select nonuniform probability samples from the cumulative distribution rather than from the complement, then the entire focus shifts to very small values of the parameter. This is the reason that each variable is permitted to have a predefined preferential direction of interest. Small values are generally of interest for particulates distributed over several decades of diameter, for example. The concept of logarithmic expansion with preferential sampling direction appears to be a very powerful approach for interrogating extreme parameter distribution tails without introducing bias to the output distribution. Additional academic investigation and practical application is needed to quantify the nonparametric convergence properties of extreme quantiles in output distributions built from finite LHS samples based on logarithmic expansion.[4]

Nonuniform probability sampling permits comprehensive interrogation of extreme tails spanning many decades of interest without introducing bias in final performance metric estimates. Unbiased estimation is achieved by carrying a local probability weight with each of the randomly generated samples. Weighted analog Monte Carlo methods

[4] Logarithmic expansion is easy to implement, but it is not the only way that nonuniform bins can be constructed to emphasize desired sampling ranges. In fact, any "elastic" functional description of probability expansion can be used to introduce nonlinear scale transforms.

are widely used in radiation transport, aerosol transport and stochastic estimation of many other natural phenomena. By analogy to a PRA event tree, each nonuniform probability weight is just a split fraction in a highly refined tree with multiple (100s to 1000s) branches per node. In contrast to a PRA event tree that follows a sequential progression of events, plant-state time variables can also be treated as random variables in CASA to proliferate a very large number of random timing sequences.

With the exception of joint frequency between break size and break location, the Year-1 version of CASA treats all random variables as independent in the same fashion as an external LHS UQ with no correlated variables. LHS is guaranteed to return an unbiased estimate of the output mean, but estimates of other percentiles may not be as accurate. In particular, estimates of the extreme tails of failure that are of interest for risk assessment may be misleading unless compensatory sampling strategies like logarithmic expansion are employed. The problem of imprecise and possibly biased estimates of extreme tails is mitigated somewhat by calculation of conditional LOCA categories that force local comparisons rather than interpretations of the entire distribution at the same time. Two improvements to pursue in the following year include (1) supporting correlations through joint sampling of more variables, and (2) further academic investigation of upper quantile convergence properties with the application of logarithmic expansion.

The generalized concept of logarithmic expansion in the nonuniform sampling scheme permits resolution to be added in parameter ranges that are of greatest concern without introducing bias to the statistics of final performance metrics. The obvious example in this problem is large DEGB breaks that have very low relative occurrence probability. Sampling on a logarithmic scale permits these rare events to be included at any desired resolution, and concurrent probability weighting prevents unbalanced representation in the final results. It is interesting to observe that with logarithmic sampling, estimates of upper quantiles in the output distributions will converge more rapidly than will central estimates like the mean, which is of little interest in this application.

The present sampling strategy assures that every weld location experiences a DEGB and a number of break events in each LOCA category that is proportional to the size of

the LOCA range. The product of the number of welds and the number of breaks per weld determines the size of the LHS design for all other independent random variables. This bottom up sampling approach ensures that all possible DEGB events are included, but it will not guarantee that maximally conservative combinations of all other variables appear in the design. Replicate evaluations of the independent LHS design are needed to assess convergence of upper percentiles on plant performance metrics. Year-2 developments may include strategies for optimizing the LHS design to better canvas the parameter space and reduce the number of brute force iterations that is needed to reach a desired accuracy of convergence.

All physical variables with random distributions are captured in a global LHS design matrix with an equal number of samples, except for debris bypass. Variability in debris bypass depends on sump flow rate that is defined uniquely at the start of recirculation. Variability in the available bypass correlation is large and yet stable estimates of failure probability induced by this phenomenon are desired, so a hybrid method referred to as "splitting" is employed in CASA to propagate a full range of 10 bypass values for *every* scenario rather than a single random value for *each* scenario. Multiplicative weights are computed as usual for the additional branches, and final distributions of deposition in fuel assemblies are properly normalized by the total probability weight of all independent scenarios.

Small, Medium and Large LOCA events are grouped for separate analyses to provide a clean interface with the external PRA. Compilation for each LOCA category is accomplished by grouping results according to the break size of their initiating event and forming conditional probability distributions of performance metrics that are normalized to the total probability weight of each subpopulation. Separate probability distributions can be specified for S, M, and L event categories for many of the random variables. This is presently the only opportunity to introduce explicit correlations between variables.

Additional initiating event sequences of interest include RCP seal LOCAs, and PRT safety relief valve (SRV) actuation related to feed-and-bleed scenarios. Selection of these events is consistent with existing transients used in the PRA. Failure probabilities for these additional initiators are presently assigned by comparison to the spectrum of

weld break results, but Year-2 improvements will include specific geometry files for these plant locations.

Because SLOCA, MLOCA and LLOCA cases are compiled separately, the desired maximum number of breaks per weld is spread in proportion to the size range of each LOCA category relative to the LLOCA range of the largest DEGB. This same approach is used to assign the number of samples to a weld with a DEGB condition that lies between LOCA categories. Thus, it is appropriate to view the maximum number of breaks per weld as a bounding sampling resolution on the very largest breaks possible in the plant. In all cases, the minimum number of breaks per weld is always 1 in every LOCA category that a given pipe can contribute to. Because the LLOCA size range is much larger than the range of the other LOCA categories, range proportional sampling creates many more LLOCA scenarios than for MLOCA or SLOCA.

National Institute of Standards and Technology reference data are used for all thermodynamic statepoints of water. For conditions above 212°F, saturation pressures are assumed and for conditions below 212°F atmospheric pressure is assumed.

CASA has the ability to convolve two uncertain logical decision criteria: (1) exceeding an NPSH threshold and (2) exceeding a fuel assembly deposition threshold. Other performance metrics of concern will be added in Year 2. The sequence of calculations leading to a decision point (and the probability weight of their associated random variables) can often propagate into additional relationships that lead to other decision points. Although variability in a logical decision criterion can be treated identically to variability in a physical variable, it is very important that random variables associated with logical decisions are not confounded with physical variables when propagating sequence probability weights. Logical variables are external to the phenomenology and apply only to discrete points in the accident sequence. Logical variables can be viewed as filters for processing physical distributions without influencing the outcome of the accident scenarios. Precautions were taken in CASA to maintain separation between physical and logical random variables.

Initial transport of debris to the strainers during pool fill was estimated by Alion Science and Technology based on ratios of pool volume to sump cavity volume. For now, it is assumed that debris attracted to the sump during pool fill is deposited

uniformly on the entire strainer area even though directed flow towards the sumps stops long before the strainers are submerged. The design of the STP strainer actually precludes directed flow towards the sumps until the pool level has reached the depth of the common header joining the strainer modules. At this point, the lower cavities will begin to fill and draw suspended debris towards the sump. For most scenarios, the fraction of debris assumed to arrive during pool fill is small compared to the total debris arriving during recirculation, and the assumption of uniform coverage generally increases the total estimated head loss compared to partial coverage of an actual strainer device, so the approximation is minor.

Time histories in CASA begin with the occurrence of the break to maintain consistency with safety evaluation calculations and EOP action times. Few predictive models of debris fate exist between the time of generation in a ZOI and the beginning of recirculation. Transport logic diagrams are generally constructed to trace plausible fractions retained on gratings, eroded from sprays, sequestered in dead cavities, etc. The basic elements of a logic diagram are specified by the user in CASA, but additional refinement and accessibility are needed.

Only two sizes of debris (large and fine) are currently tracked in CASA. Large pieces are subjected to erosion, but they do not transport during washdown. Fines are assumed to have 100% transport to the pool during washdown, then a partition among inactive sumps during fill up determines the fraction remaining for suspension and transport during recirculation. No credit is taken for settling of fines.

The current fiber bypass correlation is insensitive to break size. It depends only on velocity during initial bed formation. CASA evaluates the bypass velocity at the beginning of recirculation by adding flow rates from all operating pumps on each train. Bypass uncertainty is treated as an independent variable for compilation separate from ΔP. Because bypass quantity was added relatively recently, and because the functional dependence on velocity embeds the variation within each scenario, the strategy of “splitting" was used to append this variability to all break scenarios defined in the LHS sampling matrix.

Wide variability in estimates from the bypass correlation can lead to unrealistic estimates for bypass quantity that exceed the total fiber inventory available in the

scenario. A filter was imposed to limit bypass to the minimum of either the correlation result, or the total fiber accumulated during a user-specified window of principal penetration. (Recall that the homogeneous pool concentration is limited by the total debris inventory in the scenario). Significant fiber penetration can only occur while the strainer maintains a significant open flow area. Given that debris is double counted in CASA in the sense that debris passing through is not subtracted from debris arriving in the bed, a reasonable time window is monitored to limit total debris penetration. This window is defined specific to each LOCA category, so for example, the window can be left open indefinitely for SLOCA that may not have sufficient fiber to completely cover the active strainers.

Time and temperature dependent $NPSH_{margin}$ histories for the containment spray pumps, low-head safety injection pumps, and high-head safety injection pumps are currently constructed from pump-specific histories reported for LLOCA in Ref. (RAI response). Containment histories that are as close as possible to the random break-size scenario will eventually be selected from a library of MELCOR calculations. For now, user supplied SLOCA, MLOCA and LLOCA uncertainty factors on pool temperature and time are applied as a shift to the entire surrogate profiles to enforce time correlation and avoid erratic fluctuations during the accident scenario that would be introduced by sampling random conditions at each time step. Presently, uncertainty factors for $NPSH_{margin}$ and pool temperature are sampled independently, but an obvious correlation needs to be forced between this pair of variables. The minimum margin among the 3 safety pumps at any point in time is used as the ΔP decision criterion for possible recirculation failure.

CASA presently tracks only two debris size categories: fine and large. A more generic transport logic diagram is envisioned that will handle any number of debris sizes and transport fractionation steps. Fractionation describes the potential fate of ZOI debris components such as hold up on gratings, sequestration in dead cavities, settling in containment, etc. In a generalized transport logic diagram, the user will have to specify conditional probability distributions for all potential splits and all desired size fractions.

In the current treatment of time-dependent pool concentrations, debris source terms are limited to total instantaneous introduction at specific times. The differential equation for accumulation on the screen can be easily generalized to account for random rates of introduction for each debris component (for example, the failure rate of unqualified coatings is not instantaneous), but there was not sufficient consensus for these factors to warrant development in the initial quantification. Time-dependent debris accumulation does account for the time history of flow rate, but it does not have any information on changing pool volume or pool depth. These factors might be important for cases where pool volume continues to change after recirculation begins.

The introduction of pump-time trip points (ON or OFF) offers flexibility for tracking the effect of EOPs in combination with presumed mechanical failures and for potentially optimizing EOP actions in the future. Time-trip points are always defined as separate random variables for SLOCA, MLOCA and LLOCA. CASA results are almost exclusively driven by flow demand at the strainers, and runout flows are assumed for all operating pumps. Standard pump trip to start flow include: (1) the time to begin recirculation, (2) the time to turn on spray, (3) the time for low-head pumps to inject significant volume flow.

CASA presently offers three options to turn off pumps at random times, but only if ALL trains are available from the outset of the scenario. Discretionary actions to turn off pumps include: (1) *one* spray pump off, (2) *all* high-head pumps off, (3) *one* entire train off (never used). Changing flow on any one train creates 2 possible flow histories across the available trains; full flow and partial flow. Total flow across all operating strainers controls pool debris concentrations, but individual sump flow dictates head loss and bypass across the strainer in question. Total bypass across all operating trains is summed and diversion of debris to containment spray is accounted for. Improvements planned for Year 2 include separate operations histories for each of the 9 safety pumps. This will enable a much deeper linkage with the PRA by introducing the flexibility to track combinatoric mechanical failure conditions, and high-fidelity EOP tracking including both operator error and discretionary actions.

Primary debris bypass occurs within a relatively short time period before a debris bed forms to obstruct further penetration. This window is captured by the parameter

Tbypass. If pump flow modifications occur within this window following Trecirc caused by random timing trips, they are presumed to maximize flow and enhance bypass. Some limited data exist for flow rates in a fuel assembly under both conditions with and without chemicals. The data support credit for additional margin while defining two separate thresholds of concern: 75 g/FA for all CL breaks with chemicals present and 150 g/FA for all HL breaks without chemicals present. CASA presently does not know how to distinguish HL/CL locations, so a separate analysis was performed for each threshold and the results were arithmetically averaged (assumed 50/50 split between HL and CL breaks over all sizes) before reporting the results for PRA evaluation.

Chemicals that arrive at the sump can only induce severe head loss on a fully covered strainer. A criterion of 1/8-in. uniform loading is used as an operational definition of complete coverage. For times when the bed has less than this equivalent amount of fiber, no chemical bump-up factor is applied. For times greater than the initial assumed arrival of chemicals when the bed does contain more than a 1/8-in. layer of fiber, head-loss estimates were increased by a factor of 2. STP specific strainer testing supports an increase of this magnitude for use in the initial quantification.

Chemical effects from aluminum corrosion (if they occur) in the STP containment, are not expected until sometime later in the accident sequence. Chemical effects may not appear for many days, but for purpose of the initial quantification, they were assumed to be present at 24 hours. The flow condition through the core determines the threshold of concern for incore debris deposition. Five and ½ hours after recirculation starts, operators switch from cold-leg injection to hot-leg injection. Cold-leg injection is susceptible to drawing chemicals and debris through the core, but HLI is not.

Physical Assumptions:

(1) rated volumetric flow of the pumps does not depend on temperature,

(2) all operating sumps are identical and they split the debris in proportion to their respective flow volume,

(3) loss of effective area from miscellaneous debris has a minimal effect on bed thickness for a given debris volume,

(4) all debris is homogenized in the bed at every point in time,

(5) many beds are dominated by particulate, in which case, compressibility was set to the particulate packing density (Eq. B-27b in Ref. 8).

(7) for temperatures above boiling, assume vapor pressure in containment (only affects extraction of water properties, no credit presently taken for overpressure),

(8) for temperatures below boiling, use atmospheric pressure (only affects extraction of water properties).

Time Dependence

A containment accident sequence describes an inherently time-dependent scenario that progresses as debris forms, transports and accumulates during various plant states that dictate changing volumetric flow rates through the sump strainers. Volumetric flow rate determines (1) the rate of debris accumulation on any single strainer, (2) the cumulative fiber bypass through all strainers (as predicted using the bypass correlation), (3) the resistive head-loss through a debris bed, and (4) the dynamics of pool turnover, including suspended debris concentrations. Arrival of various debris types into the pool is similarly time dependent, because each source term has a characteristic failure mode and transport history. Consider, for example, the gradual formation of a chemical product compared to the rapid mobilization of latent debris under containment spray. Debris-type histories are superimposed on the plant response that defines temperature and flow rates as a function of time. System vulnerability to debris effects changes during the course of the accident transient (like $NPSH_{margin}$), so timing is an essential perspective of a comprehensive risk assessment.

CASA permits separate time-dependent flow rates from up to three safety trains and time-dependent debris introduction rates to interact and form time-dependent debris bed compositions. It is presently assumed that any debris entering the pool is instantly mixed uniformly throughout the water volume. This approximation generally ignores opportunities for debris settling and guarantees that suspendable debris types will eventually reach the screen. As long as safety margins are not challenged by “crisis points” caused by the order and exact arrival timing of debris types, the homogeneous pool approach provides valuable insights for understanding the tradeoffs between

debris accumulation and system flow dynamics. The assumption of well-mixed pool concentrations is commensurate with the present treatment of debris beds as fully homogenized for the purpose of head-loss estimation.

In the present implementation, only pool concentrations and debris-bed composition are treated as time-dependent locations for debris to reside. No credit is taken for time-dependent buildup that might occur within the core. This approximation creates a conservative contradiction whereby *all* debris arriving at a strainer is assumed to be retained in the bed with 100% filtration efficiency, *and* any debris predicted to bypass the screen at the start of recirculation is assumed to deposit entirely in the fuel channels with no bypass and no circulation back to the pool. This year-1 simplification essentially counts the bypass debris twice, allowing it to contribute to both safety concerns.

CASA tracks the mass of each debris type m_i in the pool using a first-order rate equation with nonconstant coefficients,

$$\frac{dm_i}{dt} = S_i(t) - \frac{Q(t)}{V(t)} m_i \qquad \text{Eq. 1}$$

where $Q(t)$ is the total volumetric flow rate through all active strainers {m³/s}, $V(t)$ is the dilution volume of the pool {m³}, and $S_i(t)$ is the source rate of the debris type into the pool {kg/s}. Before recirulation while $Q(t) = 0$, debris arriving in the pool is added to the total concentration of debris suspended at the time recirculation starts. The ratio Q/V {s} is the time needed to circulate the entire pool, but in Eq. 1, this period can vary during the course of the scenario.

The general solution for Eq. 1is found by introducing an exponential factor to make the equation a perfect differential that can be formally integrated; the result is

$$m_i(t) = \exp\left[-\int_0^t \frac{Q(t')}{V(t')} dt'\right]\left\{m_0 + \int_0^t S_i(t') \exp\left[\int_0^{t'} \frac{Q(t'')}{V(t'')} dt''\right] dt'\right\}. \qquad \text{Eq. 2}$$

If the initial quantity of each debris type is zero and the total anticipated quantity of debris S_0 {kg} arrives in the pool at a discrete time, then

$$m_i(t) = S_0 \exp\left[-\int_0^t \frac{Q(t')}{V(t')} dt'\right]. \quad \text{Eq. 3}$$

Mass accumulates on the debris bed at a rate of $d_i = (m_i/V)Q$, so the cumulative mass on the bed at any time is

$$D_i(t) = S_0 \int_0^t \frac{Q(t')}{V(t')} \exp\left[-\int_0^{t'} \frac{Q(t'')}{V(t'')} dt''\right] dt'. \quad \text{Eq. 4}$$

The integrals in Eq. 4 are approximated by assuming the pool turnover period is constant during small intervals of time Δt. CASA can easily be generalized to accept time-dependent rates of debris introduction, but for now, only discrete batches of debris can be added at specific time points.

Pool concentrations are affected by the total flow rate drawn collectively through all of the active strainers, but for the purposes of bed formation, debris arriving at the sump is distributed to each active strainer in proportion to their local flow volume.

Initial Results

This section presents a selection of results from CASA to illustrate some of the input assumptions and also the nature of the results that are generated. Graphic representations of the calculation are useful for spotting anomalies that would otherwise be missed.

Figure 15 illustrates an example function of $NPSH_{margin}$ for the low-head safety injection pump that was adopted from Ref. (RAI response). The presentation is a bit nontraditional because the dependent variable (NPSH) is shown on the horizontal axis as a trend line of two separate independent variables (time and temperature). As expected, $NPSH_{margin}$ increases rapidly with increasing time (green line from left to right) and increases with decreasing temperature (blue line from left to right).

After sampling thousands of possible break scenarios as described in Section: Sampling Strategy for Weld Breaks, the individual break sizes (and their corresponding probability distributions) can be organized into a complementary cumulative distribution function (CCDF) like those shown in Figure 16. (A CCDF reports on the vertical axis the probability of exceeding a value of interest on the x axis). Twenty-five

replicates of ~3000 samples each are superimposed to illustrate the degree of variability across the spectrum. By design, the extreme DEGB conditions are characterized more accurately than the less interesting SLOCA events.

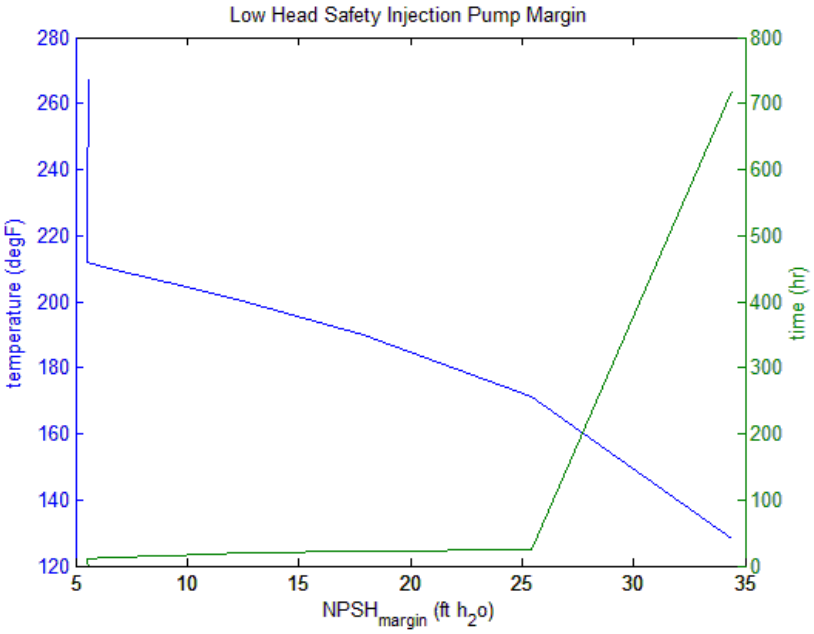

Figure 15. Example $NPSH_{margin}$ curve for low-head safety injection.

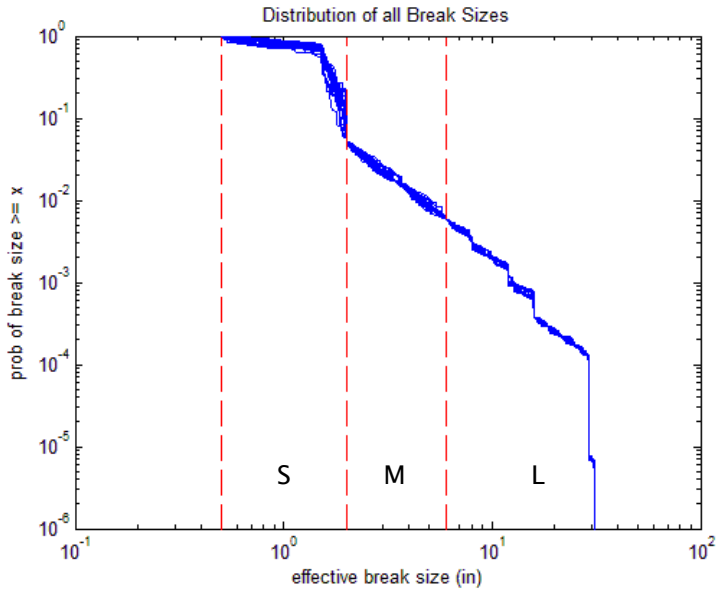

Figure 16. Distribution of break sizes for 25 replicates of ~3000 samples.

In some respects, fiber debris volume is the most important attribute in judging the potential severity of a LOCA scenario, because deposited fiber creates an opportunity for filtration of other debris products. The volume of fiberglass in the pool also contributes leaching products to the chemical constituents in the pool. Figure 17 illustrates CCDFs for 3 independent replicates of ~3000 samples each. SLOCA events represent the predominant accidents, so there is less than 1% chance of generating more than ~60 ft^3 of fiber in the ZOI (see marked example). On the other hand, the most extreme DEGB conditions can generate assumed quantities exceeding 3000 ft^3 of fiber. Remember that presently assumed 17-D ZOI neglect pipe whip restraints and truncation by concrete boundaries.

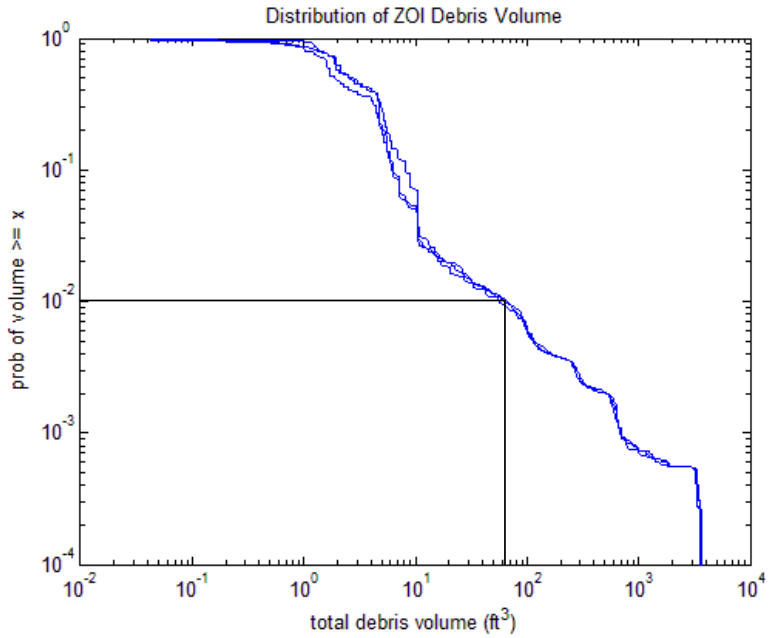

Figure 17. Distribution of possible fiber debris volume at STP.

Suspended debris arrives on the strainers over the course of time and induces time-dependent head loss. Figure 18 illustrates a few of these strainer head-loss histories for an analysis with no assumed chemical effects. Histories with an assumed chemical bump up factor of 2 raise the maxima by a factor of 2. Major features of these head loss histories include the step reduction at 600s when one spray train is turned off and a very sharp rise in head loss at 24 hr when failed coating particulates begin to arrive at the strainer. For a single CASA replicate there will be ~3000 time histories that have

been evaluated at the same list of times. The set of ΔP values at each time point is used to construct the time-dependent probability of exceeding $NPSH_{margin}$, but no cases for any size break were found that exceed the curves shown in Figure 15, even with an assumed chemical effects factor of 2. The reason that no head-loss failures are observed is because peak estimated ΔP occurs after at least 24 hrs and minimum margin exists very early in the transient.

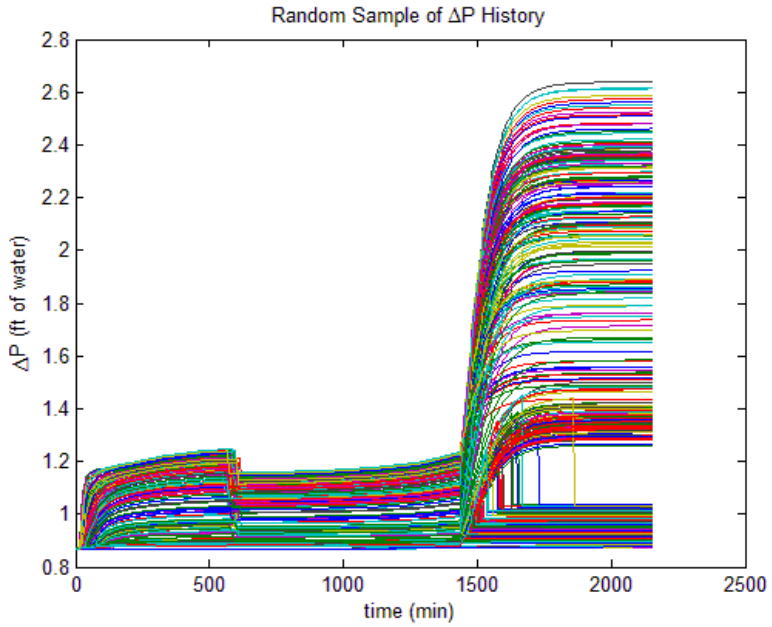

Figure 18. Sample selection of head-loss histories (without chem effects).

Debris that passes through the strainer is assumed to deposit completely and uniformly in the core. Figure 19 presents a set of 25 CCDF for fuel assembly fiber loadings in the case when only one safety train is available. As the assumed tolerance for incore fiber deposition changes (dashed line), the fraction of cases that exceed the level of concern also changes. The process for determining the failure probability with and without uncertainty in the threshold is described in Section: Estimation of Failure Probability. The maximum amount of bypass with 3 trains running is basically 3 times higher than for a single train, so if debris bypass continues to be a major concern, there is a clear incentive to reexamine LOCA response water management strategies.

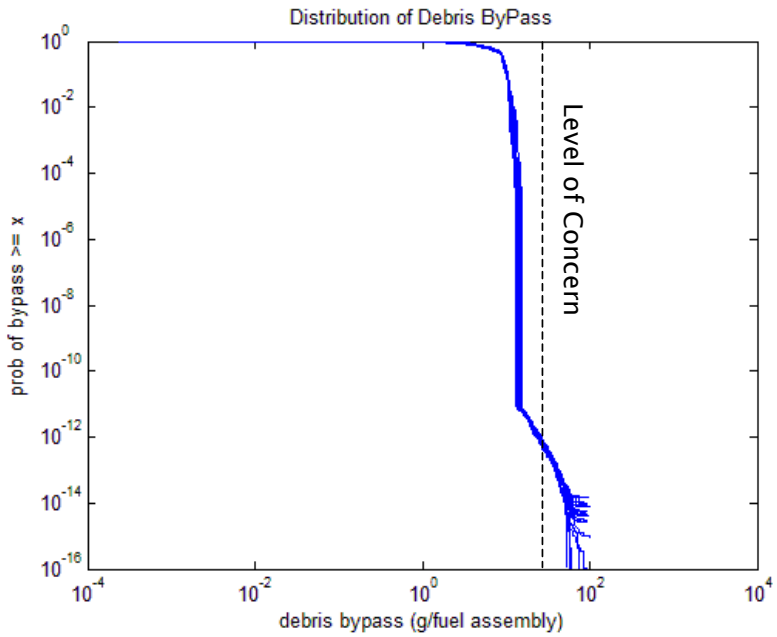

Figure 19. Distribution of debris bypass (g/FA) for one safety train.

Any of the CCDF results can be recreated using subpopulations of breaks belonging to each of the three LOCA size categories (S, M, L). These probability distributions are "conditioned" on the membership of each scenario being in the category of interest, but the process for determining failure probability (number of events exceeding threshold) is identical. To establish a convenient interface with the STP PRA for year 1, SLOCA, MLOCA and LLOCA were separated for each of three plant conditions investigated: one train operable, two trains operable, three trains operable. Twenty-five CASA replicates were found to provide reasonably accurate estimates of mean failure probability within a practical time, and two discrete fiber thresholds of 75 g/FA and 150 g/FA were imposed in separate batch evaluations. Table 3 and Table 4 present the compiled results.

In general, SLOCA events never exceed the threshold of concern because of low sump flow rates in the absence of containment spray. Failures in MLOCA and LLOCA scenarios decrease with decreasing number of operable trains, and because the number of failure events is small, the standard error on the mean failure can be large. Additional resolution and/or additional replications would be needed to achieve tighter failure estimates, but the mean values are quite low for these already low-frequency

scenarios. It should be noted that all replicates are pooled to achieve the best possible estimate of the mean and that the standard error of the mean scales as $1/\sqrt{M}$ where M is the number of replicates. Thus, 4 times more replicates are needed to reduce the standard error by a factor of 2.

Table 3. Estimated recirculation failure probability with fuel deposition threshold of 75g/FA applicable for cold-leg breaks (25 repetitions).

Ntrain = 3				
overall	small	med	large	
3.5588e-013	0	1.7878e-002	2.4545e-001	mean
9.1785e-015	0	5.8282e-004	1.2996e-003	std dev
2.5791e+000	NA	3.2600e+000	5.2948e-001	std err (%)
Ntrain = 2				
overall	small	med	large	
1.1148e-013	0	4.8313e-003	1.1726e-001	mean
7.1540e-015	0	4.4504e-004	1.7875e-003	std dev
6.4173e+000	NA	9.2116e+000	1.5244e+000	std err (%)
Ntrain = 1				
overall	small	med	large	
3.5000e-016	0	0	1.1649e-003	mean
7.2124e-017	0	0	2.4005e-004	std dev
2.0607e+001	NA	NA	2.0607e+001	std err (%)

Table 4. Estimated recirculation failure probability with fuel deposition threshold of 150 g/FA applicable for hot-leg breaks (25 repetitions).

Ntrain = 3				
overall	small	med	large	
1.3407e-015	0	0	4.4623e-003	mean
9.4499e-017	0	0	3.1452e-004	std dev
7.0485e+000	NA	NA	7.0485e+000	std err (%)
Ntrain = 2				
overall	small	med	large	
2.6345e-016	0	0	8.7685e-004	mean
5.4923e-017	0	0	1.8280e-004	std dev
2.0848e+001	NA	NA	2.0847e+001	std err (%)
Ntrain = 1				
overall	small	med	large	
0	0	0	8.7685e-004	mean
0	0	0	1.8280e-004	std dev
NA	NA	NA	2.0847e+001	std err (%)

Section: Chemical Effects Summary explained that two discrete thresholds of 75 and 150 g/FA apply to CL and HL breaks, respectively. For the purpose of initial quantification, the arithmetic average of failure probabilities from Table 3 and

Table 4 was computed to enforce an assumed equal probability of breaks occurring on either the hot or cold-leg sides of the RCS. Table 5 summarizes the composite failure probabilities that were reported to the PRA for compilation of $\triangle$CDF and $\triangle$LERF impacts caused by recirculation failure.

Table 5. Average recirculation-failure probability assuming equal proportion of cold-leg and hot-leg breaks.

	all sizes combined	small	med	large
Ntrain = 3	1.7861e-013	0	8.9390e-003	1.2496e-001
Ntrain = 2	5.5872e-014	0	2.4157e-003	5.9068e-002
Ntrain = 1	1.7500e-016	0	0	5.8245e-004

In Year 1, CASA development focused heavily on building the mechanics needed to process weld-rupture ZOI events. Other initiators that can require recirculation through the containment sump include reactor coolant pump (RCP) seal leaks and transients involving the pressurizer relief tank (PRT). Explicit geometry files will be constructed in Year 2 for these specialized break locations, but for the initial quantification, insights gained from the weld rupture spectrum were used to assess recirculation failure for the other initiators. In particular, because (1) no weld breaks were found that challenge $NPSH_{margin}$ based on debris volume, and (2) RCP events initiate a plant response similar to SLOCA with no spray, it was recommended to the PRA that there be *no increase* in recirculation failure caused by RCP-related accident scenarios. Similar logic applies to PRT rupture-disk events, but in addition, there are no insulation targets near the PRT that can contribute to debris generation. It was recommended that there be *no increase* in recirculation failure caused by PRT-related accident scenarios.

Probabilistic Risk Analysis

Probabilistic Risk Assessment (PRA) provides a logical framework to integrate the results of the analyses being performed to explore the risk-informed resolution of GSI 191. Key metrics of interest provided by the PRA are Core damage frequency (CDF) and large early release frequency (LERF). In addition, the PRA provides insight into the contributors to individual sequences, or groups of sequences, of interest.

The 2011 effort built on the foundation provided by the PRA Model of Record (MOR) at STP. While the MOR does explicitly include consideration of sump blockage during

recirculation, modest changes were made to the MOR logic models. These changes were made to facilitate the assignment of different sump plugging likelihoods for specific scenarios and to add representation of so-called 'downstream' scenarios into the logic model. These downstream scenarios represent the potential for fuel channel plugging due to material bypassing the strainers. Such scenarios were not previously considered in the MOR.

STP Model of Record

The STP MOR model name is STP_Rev6. The MOR does explicitly consider the possibility of sump strainer blockage resulting in recirculation failure. The concern is that excessive blockage could result in the loss of NPSH for pumps during recirculation, leading to loss of flow.

No plant-specific analyses were performed to support the sump strainer blockage likelihood. Rather, a generic likelihood representing sump blockage failure was assigned from the PLG generic database. That likelihood was derived by an expert panel convened in the 1990s in response to the 1992 Barsebäck unit 2 partial strainer blockage event. The mean value of that likelihood is 1E-5. This value is applied to all scenarios involving recirculation in the MOR. The 1E-5 value was also used as a default value for sump blockage following RCP seal LOCAs and small LOCAs in a 2009 Westinghouse report (WCAP-16882-NP). The Westinghouse report suggested larger values (1E-4 to 1E-3) for LOCAs whose location could result in more insulation material being damaged and for larger LOCAs. Strainer blockage in the MOR is represented by a single basic event located in the system fault tree and results directly in the failure of all three trains in recirculation.

The MOR, however, does not explicitly address flow blockage events that could result in material bypassing the strainers.

The contribution to core damage frequency due recirculation failure (from all causes, not limited to sump blockage) is reported below in

Table 6.

Table 6. Contribution to core damage frequency from all causes as assumed by STP model of record.

Initiator Category	Initiator Frequency (yr-1)	Sump Blockage Likelihood	CDF due to Recirculation Failure
RCP Seal LOCA	2.38E-3	1E-5	2.59E-8
Non-Isolable Small LOCA			
Medium LOCA	4.96E-4	1E-5	9.05E-10
Large LOCA	2.66E-5	1E-5	6.34E-11
Other events including transients	2.67E-6	1E-5	2.38E-11
Total	--	1E-5	2.03E-10
	--	--	2.73E-8

The results from the MOR suggest that the frequency of recirculation failure resulting in core damage is on the order of 3E-8 per reactor calendar year and the largest contribution is from RCP Seal LOCA. Medium and Large LOCAs are very small contributors to the frequency of core damage due to recirculation failure. This result is not surprising because the same likelihood for sump blockage (1E-5) is used for all initiators and the frequency of recirculation demand, as modeled in the MOR, is significantly higher for RCP Seal LOCA than for Medium or Large LOCAs.

Note that the truncation frequency for the MOR is 1e-12.

PRA Model Changes to Reflect New Analyses

Two key modifications were made to the MOR to incorporate the results of plant-specific analyses supporting resolution of GSI 191. The first of these logic model structure changes was to remove the sump blockage likelihood from the recirculation fault tree and assign it to a separate top event in the event tree. This change was made in anticipation that the assignment of initiator and/or scenario-specific sump strainer blockage frequencies may be necessary.

As indicated above, the MOR did not consider fuel damage sequences that were the result of fuel element blockage caused by material bypassing the strainer. A new top event in the event tree was, therefore, added to sequences involving 'successful' recirculation to reflect this phenomenon. The supporting evaluations indicate that the

likelihood of sufficient material bypassing the strainer resulting in fuel damage is both a function of the initiator and the number of trains operational.

The supporting analyses for Year 1 indicate that it is not possible to have sufficient material present to cause sump strainer blockage resulting in loss of NPSH. The updated PRA model therefore replaced the generic 1E-5 likelihood with zero.

The supporting analyses for Year 1 also indicate that it is not possible to have sufficient strainer bypass to result in fuel damage for transients, RCP Seal LOCA, Small LOCA or opening of Safety Valves resulting in recirculation. Fuel element blockage is possible for Large LOCAs and for some Medium LOCAs. The analyses suggest that no fuel blockage would occur if only one train is operating under recirculation. The conditional likelihood of fuel damage is largest for Large LOCA with three trains operational (12.5%) as presented in Table 5.

The model changes made to reflect sump and fuel element blockage phenomena are depicted in the following Large LOCA event sequence diagram (Figure 20).

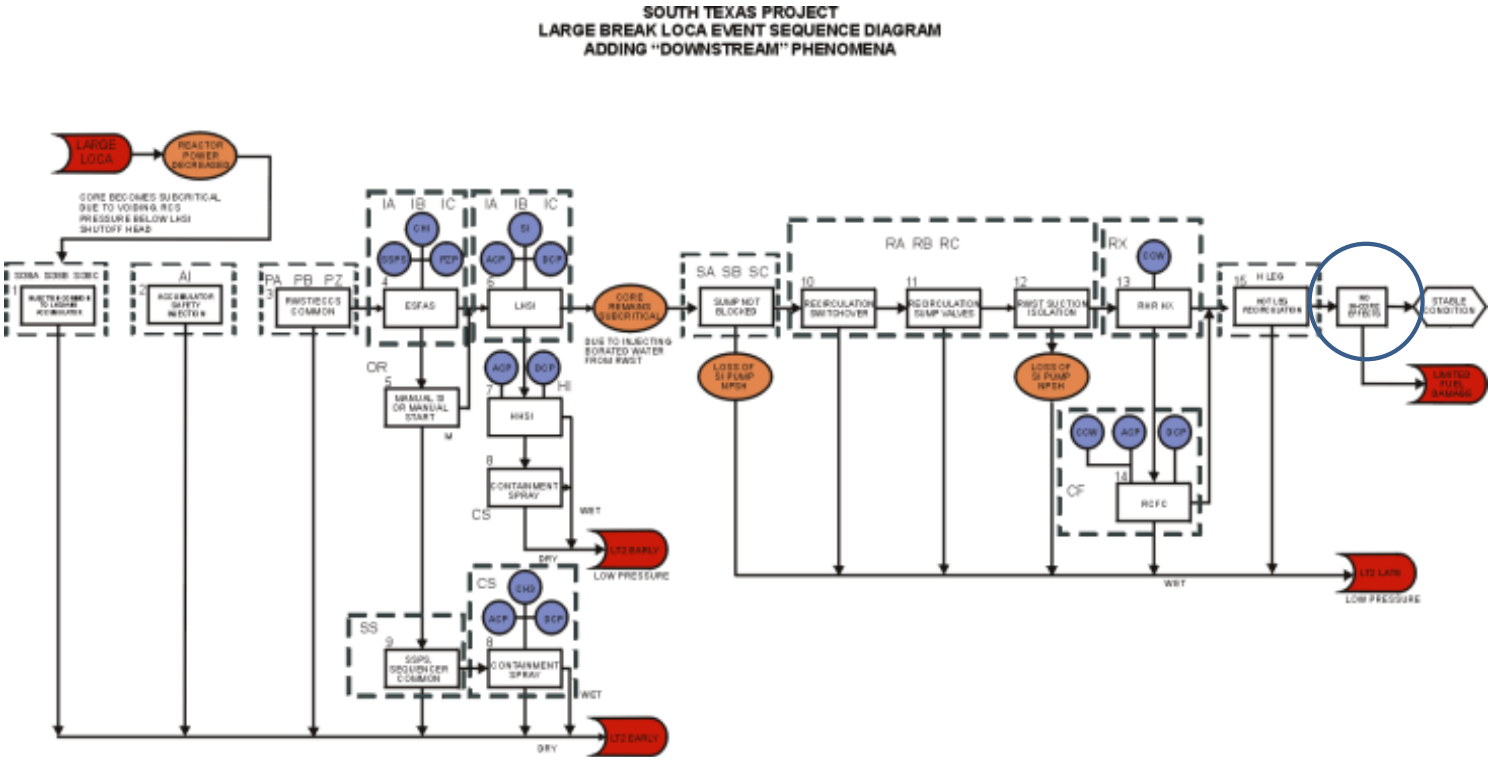

Figure 20. PRA model changes made to reflect sump and fuel element blockage.

Observations from 2011 Activities

A comparison of the CDF and LERF metrics for the MOR and the PRA model revised for this project is made in the tables Table 7 and Table 8 below.

Table 7. Baseline risk impacts from the STP model of record.

MOR: STP_Rev 6 with truncation 1E-14					
Initiator Category	Sump Blockage Likelihood	Fuel Element Blockage Likelihood	CDF w/o Fuel Element Blockage	Frequency of Fuel Element Blockage	CDF w/ Fuel Element Blockage
RCP Seal LOCA	1E-5	0	1.55E-07	0	1.55E-07
Non-Isolable Small LOCA	1E-5	0	2.76E-08	0	2.76E-08
Isolable Small LOCA	1E-5	0	2.87E-08	0	2.87E-08
Medium LOCA	1E-5	0	1.09E-08	0	1.09E-08
Large LOCA	1E-5	0	9.86E-09	0	9.86E-09
Open SRV (one)	1E-5	0	4.00E-10	0	4.00E-10
Open SRV (two or more)	1E-5	0	7.62E-11	0	7.62E-11
All other initiators	1E-5	0	6.23E-06	0	6.23E-06
Total			6.45E-06		6.45E-06
Portion of Total that is LERF			5.1349E-07		5.1349E-07

Table 8. Risk impacts from the STP modified (2011) PRA.

Current Model with truncation 1E-14					
Initiator Category	Sump Blockage Likelihood	Fuel Element Blockage Likelihood vs Number of operating ECCS Trains; 1 train/ 2 trains/ 3 trains	CDF w/o Fuel Element Blockage	Frequency of Fuel Element Blockage	CDF w/ Fuel Element Blockage
RCP Seal LOCA	0	0/0/0	1.33E-07	0	1.33E-07
Non-Isolable Small LOCA	0	0/0/0	2.68E-08	0	2.68E-08
Isolable Small LOCA	0	0/0/0	2.87E-08	0	2.87E-08
Medium LOCA	0	0/2.42E-3/8.94E-3	1.07E-08	2.11E-07	2.22E-07
Large LOCA	0	5.82E-4/5.91E-2/1.25E-1	9.82E-09	2.97E-07	3.06E-07
Open SRV (one)	0	0/0/0	3.89E-10	0	3.89E-10
Open SRV (two or more)	0	0/0/0	6.65E-11	0	6.65E-11
All other initiators	0	0/0/0	6.22E-06	0	6.22E-06
Total			6.43E-06		6.94E-06
Portion of Total that is LERF			5.1349E-07		5.1380E-07

Both models were quantified using a 1E-14 truncation to reduce the chance that small changes are not underestimated.

The current model yields significant insights. First, blockage of the strainers sufficient to cause loss of NPSH is not predicted at STP. Second, transients involving recirculation, small LOCAs and SRV opening do not contribute to fuel blockage due to material that bypasses the strainers. Third, the dominate mechanism leading to fuel damage for Medium and Large LOCAs is due to fuel blockage by material bypassing the strainer and not by sump strainer blockage.

While the detailed results differ from those of the MOR, the change in CDF and LERF are small. The PRA model incorporating CASA results have continued to be reviewed and refined since the original preliminary results were derived in early December, 2011. Following these reviews, the core damage and large early release frequencies estimates were revised. The best estimate for the decrease in core damage frequency if all fibrous insulation were to be replaced with RMI is 5.1E-07 which is a slight increase in the estimate derived earlier (ΔCDF = 4.96E-07 and ΔLERF = 3.10E-10 events/yr). The estimated increase in the frequency of large early release remains well below 1E-07. The values supporting this assessment are reported in Table 8.

Path Forward

The current results provide an initial representation of sump and fuel blockage phenomena. Detailed discussions among lead analysts are necessary to assure that model interfaces are coherent, that the effects of key modeling assumptions are understood and the results of supporting analyses are well understood by other technical team members. While the architects of individual key supporting analyses have indicated that their analyses are conservative, it is only after they are viewed in an integrated fashion that we can support a conclusion that the model overall is either realistic or conservative.

A second key activity that would strengthen the analysis is to establish scenario timelines for different initiators. It is of interest to track, as a function of time, the location and amount of debris, the formulation and location of evolved chemicals, flow rates and other plant system conditions (e.g., number of operating fan coolers) as a function of time. Additional thermal-hydraulic and containment accident analyses may be required. In addition, operator input is desired to identify when specific actions

would occur and how long-term recovery is accomplished. The current model is based on the commonly assumed 24-hour nominal mission time for mitigating systems. While the representation of downstream effects is conservative in the adopted approach, it may be possible to identify, for example, the achievement of stable plant states prior to the introduction of generated chemicals. Suggestions of scenarios for detailed analyses are described in the next section.

Potential Scenarios for Further Consideration

Scenarios for 2012

1. Background

The potential impact of sump plugging and fuel flow blockage is governed by those sequences requiring recirculation from the containment sump to prevent core damage. The current South Texas Project PRA model of record (STP_REV6) identifies those sequences which require sump recirculation and currently are mapped to a successful end state. STP_REV6 was approved for use on July 30, 2009. Sequences requiring recirculation from the containment sump involve leakage from the RCS which therefore requires long term makeup to the RCS to provide fuel cooling, even after the RWST is exhausted. Recirculation from the containment sump with heat removal by RHR or containment fan coolers can provide this long term cooling required.

2. Groupings of RCS Leakages

The classes of sequences that require sump recirculation for sequence success currently modeled in the South Texas Project PRA (i.e. model STP_REV6) are:

1. RCP seal LOCAs (these include scenarios that result from failure of one RCP seal as the initiating event, and scenarios involving seal degradation in response to a fire disabling all RCS seal injection together with an independent equipment failure causing a loss of all thermal barrier cooling. (successful recirculation frequency is 2.49E-3/yr)
2. Isolable small LOCAs (ILOCA) involving leakage downstream of a pressurizer PORV block valve causing plant trip (successful recirculation frequency is 9.09E-4/yr)
3. Small LOCAs equivalent to 0.5-in. to 2-in. diameter breaks that causes plant trip (successful recirculation frequency is 4.56E-4/yr)
4. Transient-induced Pressurizer PORV LOCAs in response to another cause of plant trip (successful recirculation frequency is 3.24E-5/yr)
5. Medium LOCAs, equivalent to 2-in. to 6-in. diameter break that causes plant trip (successful recirculation frequency is 2.50E-5/yr)

6. Successful Feed and Bleed cooling with both pressurizer PORVs held open in response to a plant trip with loss of all secondary heat removal (successful recirculation frequency is 3.62E-6/yr)
7. Large LOCAs equivalent to greater than 6-in. diameter breaks that cause plant trip (successful recirculation frequency is 2.40E-6/yr)
8. Steamline Breaks Inside Containment leading to transient induced small LOCAs (successful recirculation frequency is 8.65E-8/yr)
9. Letdown Unisolated within containment but isolated from passing through containment (successful recirculation frequency is 4.08E-8/yr)
10. RCS Pressure Relief During ATWS involving both pressurizer PORVs and potentially all 3 safety relief valves opening and at least one valve not closing (successful recirculation frequency is 7.37E-9/yr)

For item 1 (RCP seal LOCAs), 87% of the successful recirculation frequency involves failure of just one RCP seal. The other 13% of the frequency largely involve failures of all 4 RCP seals concurrently as a result of a fire induced failure of all RCP seal injection. This LOCA group has a relatively high successful recirculation frequency and is therefore given higher priority for further investigation.

Item 2, isolable small LOCAs are evaluated as having a relatively high successful recirculation frequency, but the STP model of record conservatively omits credit for the operators isolating the associated PORV block valve when the end state is already mapped to success. The operators are very likely to isolate the associated block valve within the 10 hours available before sump recirculation switchover (split fraction RE1=1.67E-4) since power is available to the block valve in all the top sequences. Once credit for block valve isolation is taken, the successful recirculation frequency for this LOCA group is only 1.5E-7/yr.

For small LOCAs (item 3), two initiating events contribute; i.e. small LOCA breaks (SLOCA), and leaks through the pressurizer safety relief valves (RCRV). Only 1.5% of the frequency involves leakage through the safety relief valves. For the small LOCA breaks, all but about 6% of the sequences involve successful mitigation by 3 trains of ECCS.

For item 4 (transient induced Pressurizer PORV LOCAs), the highest frequency initiating event contributors involve loss of primary flow (25% of the frequency) or involve losses of offsite power (75% of the frequency). Losses of primary flow are more frequent initiating events but the losses of offsite power are more likely to involve an independent loss of an emergency bus that together would preclude isolation of an initially leaking PORV. Almost all of the scenarios involving loss of offsite power also involve loss of one train of ECCS, which shares a dependency on the failed emergency bus. By contrast, tree trains of ECCS are very likely to be available for the scenarios beginning with a loss of primary flow.

For item 5 (medium LOCAs), 96% of the success recirculation frequency involve breaks in the RCS (MLOCA) with the remaining 4% from a pressurizer SRV failing open. All three trains of ECCS are very likely to be available for both contributions. In each case ECCS injection flow may be directed to the broken RCS loop bypassing the core.

For item 6 (feed and bleed cooling), the effluent is directed to the PRT. Approximately 40% of the successful recirculation frequency is from a single control room fire (FR23) that disables all AFW. The remainder is split between different causes of plant trip with an independent failure of AFW. The containment fan coolers are expected to be operable to limit containment pressures below containment spray actuation. The successful recirculation frequency of this LOCA group is approximately a factor of 100 lower than that for small LOCAs. Since the effluent is also directed to the PRT, where little insulation debris would result, this group is assigned a lower priority.

For item 7 (large LOCAs), there is only one initiating event category (LLOCA) in this group. All three trains of ECCS are very likely to be available, but the ECCS flow may be directed to the broken RCS loop, bypassing the core. Though low in successful recirculation frequency, this scenario is given priority because it, along with medium LOCAs, involve the highest velocities through the sump strainers.

Of the above successful recirculation sequence groupings, items 2, 8, 9, and 10 are of such low frequency that they can be dismissed as insignificant for potential sump plugging and downstream affects. Groupings 2 and 6 are of low priority due to the limited potential to create debris via insulation failure when the egress is directed to

the PRT. The applicable procedures for the remaining groupings 1, 3, 4 and 5 are described below.

The following describes the prioritized list of scenarios for further investigation in 2012. The flow of procedures which would guide the operators is described to the extent currently known.

1. **RCP seal LOCAs (both as an initiator and as a result of seal degradation in response to loss of all seal cooling)**

RCP seal LOCAs resulting in success via sump recirculation as a sequence group involve the highest frequency of LOCAs requiring sump recirculation and ending in success; i.e. no core damage. Relative to the total CDF, such sequences are nearly 400 times as likely to occur. It is very likely that all three trains of ECCS are available to operate in such sequences. The STP_REV6 model of record does not initially distinguish when all seal cooling is lost whether the RCP seal LOCAs are very small (21 gpm per pump) from those that are large (i.e. 480 gpm per pump). However, we expect that those occurring as an initiator will yield higher initial flow rates for the single pump affected; i.e., 480 gpm per pump. For the second scenario, when all 4 pumps lose seal cooling, we assume that all four pumps begin leaking 15 minutes after the loss and each leaks at 480 gpm, as a bounding condition.

The procedures applicable to this family of RCS leakages are similar to that for small LOCAs as an initiating event.

3. **Small LOCAs (equivalent to 0.5-in. to 2-in. diameter break that causes plant trip)**

We select the upper end of the small LOCA break sizes and to place the break in the cold legs as a limiting condition. It is very likely that all three trains of ECCS are available to operate in small LOCA sequences. We assume that containment spray actuation will not occur according to MAAP (Ref. 10) provided at least one of three trains of containment fan coolers is operating. Once the small LOCA occurs, the operators would enter 0POP05-EO-EO00 REACTOR TRIP OR SAFETY INJECTION. Containment pressure is expected to remain low with the RCFCs running, so that containment spray would not be actuated (Reference 1, action HERA1). In step 14, the

operators would then transfer to 0POP05-EO-EO10, LOSS OF REACTOR OR SECONDARY COOLANT and would start monitoring the Critical safety Functions. The RCS pressure is expected to momentarily dip below 1430 psig and then equilibrate at about 1600 psig after SI actuation and with the RCS at 570F (Reference 1, action HEOD04). Per step 1 of EO10, the operators trip the RCPs. Step 10b and the conditional information page then direct the operators to close the Pressurizer PORV block valve. Since RCS pressure is less than 1745 psig, the operators would not transfer out to the SI termination procedure, instead continuing in EO10. Step 17 directs the operators to terminate LHSI flow since RCS pressure is above 415 psig. Step 21b then directs them to 0POP05-EO-ES12 POST LOCA COOLDOWN AND DEPRESSURIZATION; i.e. for smaller LOCAs . The conditional information page of ES12 directs that when RWST level drops to 75,000 gallons, the operators would transfer to 0POP05-EO-ES13, TRANSFER TO COLD LEG RECIRCULATION. For such a small LOCA, however, without spray actuation, this level would not be reached for about 10 hours, even assuming no securing of the HHSI pumps (Reference 1, action HERA1). In step 2 of ES12 the operators are directed to turn off the LHSI pumps since RCS pressure is above 415 psig. Step 3 directs that maximum charging flow be established. Step 6 directs that an RCS cooldown be initiated using the condenser or the SG PORVs limited to a rate of less than 100 °F per hour. Step 10 directs that normal spray, auxiliary spray or a pressurizer PORV be used to depressurize the RCS and restore pressurizer level to 22%. There should then be enough sub-cooling margin and pressurizer level to start a RCP, if all were tripped earlier. Step 13b then begins the SI termination, one HHSI pump at a time. The last HHSI pump can only be secured if a charging pump(s) are running. Steps 14 to 28 then continue the RCS cooldown while maintaining pressurizer level and sub-cooling margin and stopping to isolate the accumulators along the way. Step 29 directs that RHR be placed in service when RCS temperature is less than 350F and pressure less than 332 psig. SI is to be restarted if pressurizer level falls below 8% or subcooling margin falls below 35F.

5. **Medium LOCAs (equivalent to 2-in. to 6-in. diameter break that causes plant trip)**

Medium LOCAs resulting in success via sump recirculation are just 1% as frequent as those from RCP seal LOCAs. Containment spray actuation is expected. The likelihood of just two ECCS trains operating for injection is just slightly lower than that of three ECCS trains operating. The reason for this is that no credit for injection from HHSI or LHSI is assumed to the RCS if the break occurs in an RCS loop fed by one of the three trains of ECCS; i.e. 3 out of 4 chance. For purposes of determining sump recirculation flow velocities, this omission is not appropriate. Whether the injection flow reaches the RCS is not as relevant. In the first year quantification, we instead model that any available ECCS train does draw upon the sump; i.e. regardless of whether the injection flow is directed out the break. Since containment spray would not be reduced initially, we instead believe that 3 trains of ECCS flow at the time of sump recirculation are much more likely.

Once the Medium LOCA occurs, the operators would enter 0POP05-EO-EO00 REACTOR TRIP OR SAFETY INJECTION. With containment pressure expected to quickly exceed 9.5 psig, they would then stop all RCPs (step 6d or step 10 when RCS pressure falls below 1430 psig, Reference 1, action HEOR08). The operators would then transfer to 0POP05-EO-EO10, LOSS OF REACTOR OR SECONDARY COOLANT and would start monitoring the Critical safety Functions.

Per the Conditional Information Page of EO10, one train of spray would be initially secured to conserve RWST inventory. Further, step 16 of EO10 directs the operators to stop all spray once containment pressure falls below 6.5 psig if the TSC concurs. However, the note before step 16 indicates that containment spray may have to run for 6.5 hours to remove iodine to support control room habitability. For Medium LOCAs this minimum run time may or may not apply since any releases to the containment are expected to be minor. We assume they would be minor and that spray termination would occur as soon as the low radiation levels can be confirmed. Therefore, the remaining two trains of spray would likely be manually terminated within say 2 hours; i.e. prior to the time of recirculation switchover. When RWST level drops to 75,000 gallons, the operators would transfer to 0POP05-EO-ES13, TRANSFER TO COLD LEG RECIRCULATION.

ES13 also directs the operators to secure one train of containment spray if all three are running and to not align more than 2 spray trains for recirculation. If no spray trains are running at the time of recirculation switchover, none are to be aligned for spray

recirculation. For medium LOCAs, all containment spray trains could be secured prior to the time to transfer to recirculation. In step 8 of ES13, the operators are also instructed to commence makeup to the RWST. After the transfer to recirculation, the operators are directed back to EO10.

In step 28 of EO10, the operators are instructed to align for hot leg recirculation after 5.5 hours and to transfer to 0POP05-EO-ES14, TRANSFER TO HOT LEG RECIRCULATION. Note that this is well after spray termination. One train of SI (i.e. HHSI and LHSI) is to be left aligned for cold leg recirculation as a caution against the LOCA having occurred in a hot leg. After switching to hot leg recirculation, the operators are directed back to EO10.

Step 29 of EO10 then directs the operators to align RHR while LHSI continues, if the TSC concurs.

6. Large LOCAs (equivalent to greater than 6-in. diameter break that causes plant trip)

Large LOCAs resulting in success via sump recirculation are just 0.1% as frequent as those from RCP seal LOCAs. Containment spray actuation is expected. The likelihood of just two ECCS trains operating is just slightly lower than that of three ECCS trains operating. The reason for this is that no credit for injection from HHSI or LHSI is assumed to the RCS if the break occurs in an RCS loop fed by one of the three trains of ECCS; i.e. 3 out of 4 chance. For purposes of determining sump recirculation flow velocities, this omission is not appropriate. Whether the injection flow reaches the RCS is not as relevant. In the first year quantification, we instead model that any available ECCS train does draw upon the sump; i.e. regardless of whether the injection flow is directed out the break. Since containment spray would not be reduced initially, we instead believe that 3 trains of ECCS flow are much more likely.

Once the Large LOCA occurs, the operators would enter 0POP05-EO-EO00 REACTOR TRIP OR SAFETY INJECTION. With containment pressure exceeding 9.5 psig very quickly, they would then stop all RCPs (step 6d or step 10 when RCS pressure falls below 1430 psig, Reference 1, action HEOR08). At step 14 the operators would then transfer to 0POP05-EO-EO10, LOSS OF REACTOR OR SECONDARY COOLANT and start monitoring the Critical safety Functions.

Per the Conditional Information Page of EO10, one train of spray would be initially secured to conserve RWST inventory. Further, step 16 of EO10 directs the operators to stop all spray once containment pressure falls below 6.5 psig if the TSC concurs. However, the note before step 16 indicates that containment spray may have to run for 6.5 hours to remove iodine to support control room habitability. For Large LOCAs this minimum run time appears to apply since some minor release is expected. Therefore, the remaining two trains of spray would likely be manually terminated only after 6.5 hours. When RWST level drops to 75,000 gallons, the operators would transfer to 0POP05-EO-ES13, TRANSFER TO COLD LEG RECIRCULATION.

ES13 also directs the operators to secure one train of containment spray if all three are running and to not align more than 2 spray trains for recirculation. If no spray trains are running at the time of recirculation switchover, none are to be aligned for spray recirculation. However, for large LOCAs, two spray trains are likely to be left running for 6.5 hours which is much later than the expected time to transfer to recirculation. In step 8 of ES13, the operators are also instructed to commence makeup to the RWST. After the transfer to recirculation, the operators are directed back to EO10.

In step 28 of EO10, the operators are instructed to align for hot leg recirculation after 5.5 hours and to transfer to 0POP05-EO-ES14, TRANSFER TO HOT LEG RECIRCULATION. Note that this is prior to spray termination at 6.5 hours. One train of SI (i.e. HHSI and LHSI) is to be left aligned for cold leg recirculation as a caution against the LOCA having occurred in a hot leg. After switching to hot leg recirculation, the operators are directed back to EO10.

Step 29 of EO10 then directs the operators to align RHR while LHSI continues if the TSC concurs.

In both the STP model of record and in the model revised for this first year quantification, two viable cooling options have been conservatively omitted from consideration. Both options would eliminate the need for sump recirculation in selected scenarios. These two alternative cooling options are:

- to provide makeup to the RWST and to continue injection into the RCS so that recirculation from the sump is not required.

- to cooldown and depressurize the RCS to sufficiently low pressures that leakage from the RCS becomes minimal, obviating the need for continued injection prior to exhausting the RWST. Decay heat is then removed via the steam generators or via closed loop RHR. Both of these alternatives are most viable for LOCAs of smaller sizes. For larger breaks there is less time to align for RWST makeup and the makeup rates required, just to match decay heat levels, are correspondingly larger. Continued makeup to the RWST along with injection into the RCS is problematical in that eventually the containment fills with water so that instrumentation within containment will be flooded and likely lost.

Thermal-Hydraulics Analysis

A RELAP5-3D input deck was constructed to study the thermal hydraulic system response of the STP power plant during a LOCA of different characteristics. The input file was validated by comparing the results with the STP safety reports and other data available in literature. A test matrix was defined to compute all the transient cases of interest for this project. Small and medium break size LOCA cases in cold and hot leg were executed and results were analyzed and submitted to the other teams of the project. RELAP5 was also coupled with DAKOTA (Ref. 11) to perform sensitivity analysis and uncertainty quantification and simple cases were executed.

The main purpose of the thermal hydraulic calculations required for the GSI-191 Risk Informed Closure Project is to study the response of the South Texas Project (STP) power plant during selected accident scenarios and to provide important information and boundary conditions for the development of other project models, such as the break jet boundary conditions and reactor containment calculations. The RELAP5-3D (Ref. 12) thermal hydraulic system code was selected to carry out the required calculations. RELAP5-3D is a successor to the RELAP5/MOD3 code that was developed for the Nuclear Regulatory Commission.

The activity carried out during 2011 can be summarized in four tasks as described below.

TASK 1: Data Collection and Analysis

Data describing the power plant necessary for the RELAP5 input preparation were collected from the STP database and safety reports. This required information included geometric information, such as hydraulic diameters, lengths, volumes, elevation changes etc, design data and operation procedures. The data were organized into tables for each of the main components of the power plant. Input files of other system codes such as RETRAN (Refs. 13, 14) and MAAP (Refs. 15, 16) were also used as a reference during this phase to retrieve additional information required for the input file preparation.

TASK 2: Input Preparation and Certification (Steady- State)

The steady-state RELAP5 input file of the STP power plant was constructed and verified using the design specifications provided by STP. The results of the steady-state simulation were compared with such design specifications and with the RETRAN code output. Adequate documentation was submitted to describe the methodology adopted during the input preparation (Ref. 17), providing a detailed explanation of the plant nodalization, simulation results and comparison with previous data. The certification of the steady-state input file was acquired prior to any other simulations of accident scenarios.

TASK 3: Input Refinement and Verification (Loss of Coolant Accident, LOCA)

Emergency Core Cooling System (ECCS) and system controls in the primary and secondary system were included in the RELAP5 input file to study the thermal hydraulic system response during a LOCA. Control variables were specifically developed to calculate parameters of interest such as total mass flow rates through the break, total water mass from the RWST and Time-to-Recirculation. Figure 21 shows the plant nodalization for a break located in the cold leg (1-D Core Configuration). The results for typical break sized within the small and medium range (<8") were analyzed and compared with the STP UFSAR results for the same break sizes and with other results of similar power plants available in the literature (Ref. 18).

TASK 4: Cases Execution

After interacting with the other members of the teams of the project, a test matrix was prepared in order to indentify the cases of interest and define the priority. The following table (Table 9) shows the combinations defined for 2011 and the subset of cases that were already executed and analyzed (marked with an "X").

Table 9. Thermal-hydraulics case execution matrix.

	Break Size					
	1.5"	2"	3"	4"	6"	8"
Cold Leg	x	x	x	x	x	x
Hot Leg		x				

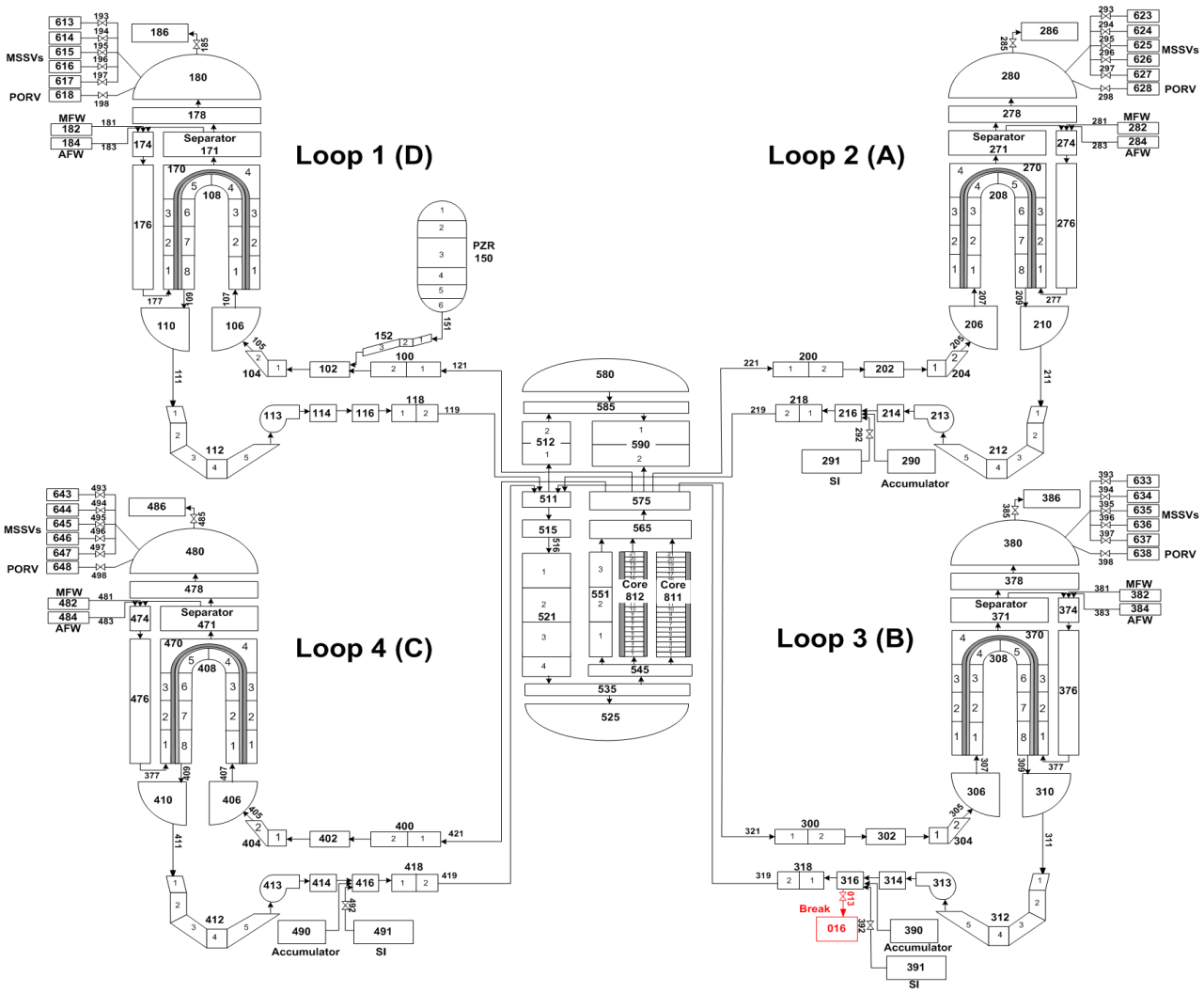

Figure 21. RELAP5 Plant Nodalization (1-D Core Configuration)

In the cold leg cases, the break was located downstream the reactor coolant pump at case approximately 12' from the reactor vessel nozzle. The break for the hot leg case was positioned at approximately 5.5' from the reactor vessel nozzle. In both cases the break was assumed to be at the bottom of the main pipe.

Additional cases of interest were also defined including additional break locations (vessel, pressurizer), different break orientations (top, bottom, lateral) and with different combinations of injection trains operating and accounting for plant operating procedures. These additional cases will be the subject of the activity during 2012.

Figure 22 provides and overview of the pressure transient in the primary system as a function of the break size for the cases listed above.

Table 10 summarizes the time-to recirculation for each cases and the final pressure achieved (one injection train only in intact loop).

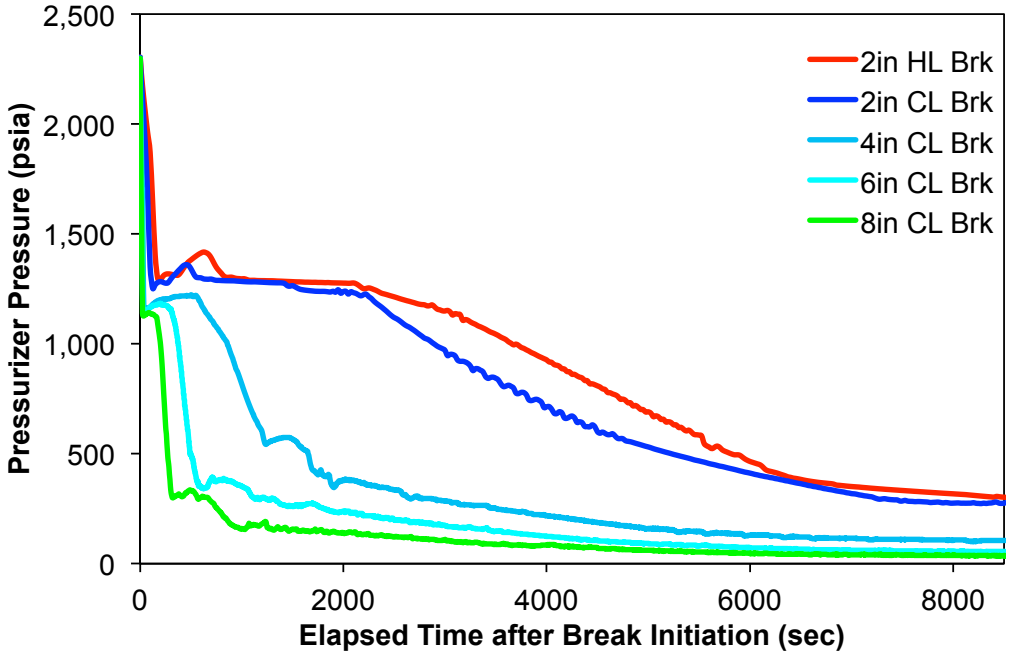

Figure 22. Simulation Results: Primary System Pressure (CL: Cold Leg; HL: Hot Leg).

Table 10. Simulation Results: Time to Recirculation and Pressure (HL: Hot Leg; CL: Cold Leg).

	Elapsed time to low-low RWST level	Primary System Pressure at this time
2inch HL	21720 s (6 h)	~ 258 psia
2inch CL	18700 s (5h 10m)	~ 281 psia
4inch CL	10500 s (2h 55m)	~ 99 psia
6inch CL	8895 s (2h 30m)	~ 54 psia
8inch CL	7860 s (2h 10m)	~ 40 psia

A detailed list of thermal hydraulic parameters was also defined and agreed with other members and data from the available simulations were extracted and provided to other teams to support activities involving the jet formation model development and the calculations for the containment.

In addition to the simulations performed with the 1-D core configuration described above, another activity was started in order to model the core and some of the vessel components (downcomer and lower plenum) using a 3-D component available in RELAP5-3D. This new node structure will help in studying the flow paths inside the reactor vessel during selected conditions under long term cooling.

RELAP5-3D was successfully coupled with DAKOTA to perform sensitivity study and uncertainty quantification. Simple cases related to the steady-state case were performed to validate the coupled software.

References

1.) STAFF REQUIREMENTS – SECY-10-0113 – CLOSURE OPTIONS FOR GENERIC SAFETY ISSUE-191, ASSESSMENT OF DEBRIS ACCUMULATION ON PRESSURIZED WATER REACTOR SUMP PERFORMANCE, Letter from Annette L. Vietti-Cook to R. W. Borchardt, SRM 10-0113, 2010.

2.) NRC, An Approach for Using Probabilistic Risk Assessment in Risk-Informed Decisions on Plant-Specific Changes to the Licensing Basis, Regulatory Guide 1.174, Revision 1, 2002.

3.) Coral Betancourt and Shawn Rodgers, South Texas Project, STP PRA Revision 6 South Texas Project Electric Generating Station Probabilistic Risk Assessment Level 1 Quantification, Revision 6.0 (Model STP_REV6), 2010.

4.) NRC, POTENTIAL IMPACT OF DEBRIS BLOCKAGE ON EMERGENCY RECIRCULATION DURING DESIGN BASIS ACCIDENTS AT PRESSURIZED-WATER REACTORS, Generic Letter 2004-02 (GL 2004-02), OMB Control No.: 3150-0011, 2004.

5.) NOC-AE-10002607, Letter from GT Powell to the USNRC, South Texas Project Units 1 and 2, Docket Nos. STN 50-498, STN 50-499, License Renewal Application, 2010.

6.) Popova E. and A. Galenko, "Uncertainty Quantification (UQ) Methods, Strategies, and Illustrative Examples Used for Resolving the GSI-191 Problem at South Texas Project", Technical Report, South Texas Project Nuclear Operating Company, December 2011.

7.) Karl N. Fleming, Bengt O.Y. Lydell, and Danielle Chrun. Development of loca initiating event frequencies for south texas project gsi-191. Technical report, 2011.

8.) Zigler, G., Brideau, J., Rao, D.V., Shaffer, C., Souto, F., and Thomas, W., "Parametric Study of the Potential for BWR ECCS Strainer Blockage Due to LOCA-Generated Debris," NUREG/CR-6224, U.S. Nuclear Regulatory Commission, Washington, DC, October 1995.

9.) Westinghouse Electric Company LLC, Evaluation of Long-Term Cooling Considering Particulate and Chemical Debris in the Recirculating Fluid, WCAP 16793-P, PWROG Project Number PA-SEE-0312, 2007.

10.) ABS Consulting, MAAP4 Analysis For the South Texas Project Electric Generating Station Probabilistic Risk Assessment Human Reliability Analysis", R-1479636-1667, prepared for STP.

11.) Adams, B.M., Bohnhoff, W.J., Dalbey, K.R., Eddy, J.P., Eldred, M.S., Gay, D.M., Haskell, K., Hough, P.D., and Swiler, L.P., <http://dakota.sandia.gov/docs/dakota/5.0/Users-5.0.pdf> "DAKOTA, A Multilevel Parallel Object-Oriented Framework for Design Optimization, Parameter Estimation, Uncertainty Quantification, and Sensitivity Analysis: Version 5.0 User's Manual," Sandia Technical Report SAND2010-2183, December 2009.

12.) RELAP5-3D User's Manual, Idaho National Engineering Laboratory, June 2005.

13.) RETRAN-3D – A program for transient thermal-hydraulic analysis of complex fluid flow systems, User's Manual, Rev. 3, September 1998 (EPRI).

14.) RETRAN Base Deck (South Texas Project Nuclear Operating Company, NC-7076 rev. 0).

15.) MAAP – Modular Accident Analysis Program for LWR Power Plants, User's Manual, November 1990 (EPRI NP-7071-CCML).

16.) Miscellaneous MAAP documents (MAAP parameter file data, figures, drawings, computation sheets, handwritten notes, calculations, etc.). All documents are organized in three volumes: Volume 1—pump parameters; Volume 2—pressurizer system, steam generator, and primary system parameters; Volume 3—RPV, steam generator, and primary system (hot leg and cold leg) parameters.

17.) RELAP5 Model Input Deck Certification – rev.3.0. STP GSI-191 Risk Informed Closure Project. Internal Documentation (2011).

18.) RELAP5 LOCA Input Certification – rev.1.0. STP GSI-191 Risk Informed Closure Project. Internal Documentation (2011).

Appendix A: CASA Grande Usage Notes

Running CASA under MatLab requires licenses for MatLab and also the Statistics and Excel Interface Toolboxes. Create a working directory for CASA Grande and use the File > Set Path option (with subdirectories) to make sure that MatLab can find all necessary subroutines and project folders. Windows 7 users may encounter file permission errors unless MatLab is invoked by right clicking on the exe icon and "running as administrator."

The user is asked to specify a master folder for defining the plant description. Usernamed subfolders then contain (1) CAD data, (2) break frequencies, and (3) storage for analytic problem variations. Any subdirectories existing below these primary paths are ignored.

Insulation data are presently provided in text files according to a standardized format. Break frequency data are presently provided in Excel files according to a standardized format. Concrete and grating data are provided in STL files. All pertinent files must reside in the user specified subfolder. All files in respective folders are concatenated into a complete geometry description. No other files may be present in the same directory. Subfolders in the path are ignored. The convenience of automatically processing multiple separate files permits flexibility in geometry development.

CAD data from the Alion data base is processed assuming the following:

(1) initial and final entries in a piping run must have zero radius of curvature.

(2) working points entered to define weld locations and hangars/valves that contain extra insulation can be essential to the piping run definitions so they should be processed along with other coordinate points.

(3) working point labels that designate break-location welds must contain the pipe i.d. and a sequence number. some flexibility is allowed for spaces and dashes but the order of the text fields must be preserved. the composite strings must match entries in a weld family correspondence table. the weld families are assigned frequency distributions as a function of break size.

(4) reactor system assignments are read from the first consequtive string of alphabetic characters in the first field of the line definition.

(5) working point labels that designate hangars, valves and nonstandard weld locations must not contain dashes. dashes are used for welds with corresponding break frequencies. synonym tables are provided for each workpoint type.

(6) miscellaneous comments regarding workingpoint labels:

- after processing, a table of misfits is provided for comparison to the list of definitions.

- all uknown label types must be resolved before analysis can proceed.

- care may be needed to avoid abbrev that match reactor system acronyms.

- to match a synonym, WP label must contain the listed abbrev and NO dashes. dashes are more generally associated with viable break locations.

- standard weld definitions resemble line i.d., usually contain dashes AND must match exactly with an entry in the weld case definition table.

(7) pipe definitions never start or end with a point having nonzero curvature, AND, intersecting tangents with nonzero curvature that define bends never have a work point assignment.

(8) locations with abrupt changes in insulation type or thickness must have colocated center points that share a common point but have separate labels. Generally, colocated points are removed unless these conditions are met.

(9) the collection of CAD files supplied to CASA must uniquely and comprehensively define all piping structures of interest. If duplicate pipe coords (defined by the concatenation of IPT and WorkPoint label) are found, a fatal error occurs. Allowing duplicate points would risk duplication of insulation volume.

Problem execution is based on a sequential processing strategy to save time on repeated variations. For example, all geometry data is read and processed only once to form a master file that can be quickly loaded. Master files for CAD, frequency and

insulation volumes are created in the user-specified casefolder. Delete any desired master file to reexecute any intermediate processing step.

Sequential listings of centerpoints and body profiles are assigned properties at discrete locations. When these properties are conferred to segment and panel interpolations, the leading point of the segment determines the property assignment.

Although LOCA size bins are somewhat standardized, CASA can parse break size data into any number of user-specified bins. A break must be >= the lower bin limit in order to be counted in the LOCA bin frequency.

User supplied break frequency data describes distribution of size for various weld types (or cases). The maximum size for each case must equal the DEGB for the corresponding pipe size. The frequency dists must be monotonically decreasing with no repeated x or y values. Cases with zero estimated weld count are immediately removed, so this could lead to unresolved CAD weld labels if indeed these cases are present.

The weld case defintion file must have column headers that include 'Line Number', 'Location' and 'Calc-Case' on the user specified tab. Other columns can be included, but only these are manipulated. The text labels must match exactly with no permissible variation. There should not be any blanks in the columns of the case definition file.

Initial CASA development centered on welds as the dominant break locations of interest, but other LOCA scenarios must also be quantified for the PRA. The proper way to use CASA for these alternatives is

(1) be sure the candidate break locations of interest are already present in the CAD files as WorkPoints with unique labels.

(2) build special break frequency and definition files just for these case studies.

(3) be sure all input parameters are tailored to the case study of interest.

If through-wall random breaks are ever investigated, modify the code to accept insulation points as the break locations. Essentially, add artificial WorkPoints

everywhere along the pipes. Will also need to tabulate total area as a basis for normalization.

Major equipment items that are insulated are approximated as axi-symmetric objects about the z-axix. Hoops of varying radii can be used to define oblique angles or to approximate curved surfaces. As with pipes, inner and outer radii define a shell of insulation. Successively replicated z-coords with shifted inner and outer radii denote an abrupt change in radius of the body. A radius of zero at the beginning or end of the object denotes a cylindrical cap at the top of the object. The z axis must be similarly duplicated wherever insulation type or thickness changes along the axis.

Major equipment is specified in the same manner as pipes except that ID and OD (diameters) become IR and OR (radii). The 'system' string present in the equip IPT field must match one of the synonyms provided for equipment labels.

Parameters that vary for S, M, and L LOCA are specified in Nloca x 1 cell arrays. Each cell can contain a full specification for a random variable.

Native unit for time is minutes, rates of debris introduction must be specified in mass/min. Units of length used in CAD data and frequency tables must be the same. Sample problem using STP data was built in inches.

Many random variables have been defined in the input deck. Some are independent of LOCA category and some are dependent on LOCA category. It is very easy to change this dependence in the code. In retrospect, all should be DEpendent, then the user can set constants if desired.

Original intent to work solely in SI units was relaxed for main program where English length and flow rates in gpm are preserved.

Count an inoperable sump as a dead cavity when assigning transport fractions T0Fract2SumpCavities and T0Fractio2DeadCavities.